

Journal Pre-proof

Calcium channel $\alpha 2\delta 1$ subunit mediates secondary orofacial hyperalgesia through PKC-TRPA1/gap junction signaling

Wen-Qiang Cui , Yu-Xia Chu , Fei Xu , Teng Chen , Lu Gao , Yi Feng , Xue-Ming Hu , Wei Yang , Li-Xia Du , Wen-Wen Zhang , Qi-Liang Mao-Ying , Wen-Li Mi , Yan-Qing Wang

PII: S1526-5900(19)30794-1
DOI: <https://doi.org/10.1016/j.jpain.2019.08.012>
Reference: YJPAI 3786



To appear in: *Journal of Pain*

Received date: 12 March 2019
Revised date: 6 July 2019
Accepted date: 6 August 2019

Please cite this article as: Wen-Qiang Cui , Yu-Xia Chu , Fei Xu , Teng Chen , Lu Gao , Yi Feng , Xue-Ming Hu , Wei Yang , Li-Xia Du , Wen-Wen Zhang , Qi-Liang Mao-Ying , Wen-Li Mi , Yan-Qing Wang , Calcium channel $\alpha 2\delta 1$ subunit mediates secondary orofacial hyperalgesia through PKC-TRPA1/gap junction signaling, *Journal of Pain* (2019), doi: <https://doi.org/10.1016/j.jpain.2019.08.012>

This is a PDF file of an article that has undergone enhancements after acceptance, such as the addition of a cover page and metadata, and formatting for readability, but it is not yet the definitive version of record. This version will undergo additional copyediting, typesetting and review before it is published in its final form, but we are providing this version to give early visibility of the article. Please note that, during the production process, errors may be discovered which could affect the content, and all legal disclaimers that apply to the journal pertain.

© Published by Elsevier Inc. on behalf of the American Pain Society

Highlights

- Infraorbital nerve injury induces primary and secondary orofacial hyperalgesia.
- *Cav α 2 δ 1* contributes to the development of secondary orofacial hyperalgesia.
- *Cav α 2 δ 1* mediates secondary orofacial hyperalgesia through PKC-TRPA1/GJ pathway.

Journal Pre-proof

Title page**Calcium channel $\alpha 2\delta 1$ subunit mediates secondary orofacial hyperalgesia through PKC-TRPA1/gap junction signaling**

Wen-Qiang Cui^{a,b,c,1}, Yu-Xia Chu^{a,b,c,1*}, Fei Xu^{c,d}, Teng Chen^{a,b,c}, Lu Gao^e, Yi Feng^{a,b,c}, Xue-Ming Hu^{a,b,c}, Wei Yang^{a,b,c}, Li-Xia Du^{a,b,c}, Wen-Wen Zhang^{a,b,c}, Qi-Liang Mao-Ying^{a,b,c}, Wen-Li Mi^{a,b,c}, Yan-Qing Wang^{a,b,c}

^a Department of Integrative Medicine and Neurobiology, School of Basic Medical Sciences, Fudan University, Shanghai, China;

^b Institutes of Brain Science, Brain Science Collaborative Innovation Center, State Key Laboratory of Medical Neurobiology, Fudan University, Shanghai, China;

^c Institutes of Integrative Medicine, Fudan University, Shanghai, China;

^d Department of Integrative Medicine, Huashan Hospital, Fudan University, Shanghai, China;

^e Department of Anatomy, School of Basic Medical Sciences, Fudan University, Shanghai, China.

¹ These authors contributed equally to this work.

* Corresponding author: Yu-Xia Chu, PhD

130 Dong'an Road, Shanghai 200032, China; yuxiachu@fudan.edu.cn

Authors' contributions

YX.C. and WQ.C. designed the experiments and wrote the paper; WQ.C., YX.C., F.X., and T.C. carried out most of the experiments and image analysis; L.G., Y.F., XM.H., W.Y., LX.D., and WW.Z. performed the experiments; QL.MY., WL.M., and YQ.W.

provided valuable advice on the research. All authors discussed the results and the manuscript.

Authors' e-mail

Wen-Qiang Cui: 16111010087@fudan.edu.cn

Yu-Xia Chu: yuxiachu@fudan.edu.cn

Fei Xu: xufeigaomi@163.com

Teng Chen: 18111010015@fudan.edu.cn

Lu Gao: lgao@fudan.edu.cn

Yi Feng: fengyi17@fudan.edu.cn

Xue-Ming Hu: 15111520028@fudan.edu.cn

Wei Yang: 16211010079@fudan.edu.cn

Li-Xia Du: 15211010072@fudan.edu.cn

Wen-Wen Zhang: 17211010072@fudan.edu.cn

Qi-Liang Mao-Ying: maoyql@fudan.edu.cn

Wen-Li Mi: wenlimi@fudan.edu.cn

Yan-Qing Wang: wangyanqing@shmu.edu.cn

Correspondence author

Yu-Xia Chu, PhD

Department of Integrative Medicine and Neurobiology, School of Basic Medical Sciences, Fudan University.

Mailing address: 130 Dong'an Road, Xuhui District, Shanghai 200032, P.R.CHINA.

E-mail: yuxiachu@fudan.edu.cn

Telephone number: +86-21-54237693

Fax: 86-21-54237611

Disclosures

This study was financially supported by the National Natural Science Funds of China (31600852, 81473749, 81771202, 81873101), the National Key R&D Program of China (2017YFB0403803), and the Development Project of Shanghai Peak Disciplines-Integrated Medicine (20180101). The authors declare that there is no conflict of interest regarding the publication of this paper.

Abstract

Orofacial pain is characterized by its easy spread to adjacent areas, thus presenting with primary hyperalgesia (hypersensitivity at the site of injury) and secondary hyperalgesia (extra-territorial hypersensitivity outside the injured zone). However, the mechanisms behind the secondary hyperalgesia are poorly understood. In the present study, we used a mouse model of partial transection of the infraorbital nerve (pT-ION) to study whether calcium channel subunit $\alpha 2\delta 1$ (Cav $\alpha 2\delta 1$) and its downstream signaling contributes to the development of secondary hyperalgesia in the orofacial area. pT-ION caused primary (V2 skin) and secondary (V3 skin) hyperalgesia, which was reversed by the Cav $\alpha 2\delta 1$ antagonist gabapentin and by the expression of Cav $\alpha 2\delta 1$ -targeting interfering RNA in trigeminal ganglion (TG)-V3 neurons. pT-ION induced increased expression of PKC and TRPA1, which was reversed by Cav $\alpha 2\delta 1$ -targeting interfering RNA, and PKC inhibition reversed the upregulation of TRPA1 and gap junction (GJ) proteins induced by pT-ION. Cav $\alpha 2\delta 1$ overexpression in TG-V2 neurons induced the upregulation of PKC, TRPA1, and the GJ proteins in the TG and trigeminal subnucleus caudalis and induced hypersensitivity in the V3

skin area, which was reversed by TRPA1, GJ, or PKC blockade. Thus, we conclude that Cav α 2 δ 1 contributes to the development of secondary hyperalgesia through its downstream PKC-TRPA1/GJ signaling pathways.

Perspective: This study demonstrates that the activation of Cav α 2 δ 1 and the downstream PKC-TRPA1/GJ signaling pathway contributes greatly to trigeminal nerve injury-induced secondary mechanical and cold hyperalgesia. This suggests that inhibitors of Cav α 2 δ 1, TRPA1, or GJs might be effective treatments for nerve injury-induced spreading of orofacial pain.

Keywords

α 2 δ 1 subunit, orofacial pain, transient receptor potential ankyrin 1, connexin, trigeminal ganglion

Introduction

Chronic pain is a common clinical syndrome that has significant negative effects on quality of life and leads to enormous social and economic problems, and among chronic pain conditions orofacial pain can be the most severe and debilitating^{41, 50}. Such pain can derive from orofacial inflammation and tissue and nerve injuries and is characterized by primary mechanical hyperalgesia (hypersensitivity at the site of injury) and secondary mechanical hyperalgesia (extra-territorial hypersensitivity outside the injured zone)^{40, 47}. In addition, hypersensitivity to cold stimulation is very commonly reported and considered to be among the most severe symptoms suffered by orofacial pain patients. The molecular mechanisms responsible for the secondary

hyperalgesia, especially cold hypersensitivity, remain unknown, and this has severely limited the development of specific and effective treatments for chronic orofacial pain.

The calcium channel subunit $\alpha 2\delta 1$ (Cav $\alpha 2\delta 1$) is a structural subunit of the voltage-gated calcium channels (VGCCs)¹³, and Cav $\alpha 2\delta 1$ in the spinal cord and dorsal root ganglion plays a key role in the processing of neuropathic pain^{5, 23, 30}. Luo et al. found that chronic constriction injury of the infraorbital nerve (CCI-ION)-induced Cav $\alpha 2\delta 1$ up-regulation might contribute to orofacial neuropathic pain through improper formation of excitatory synapses and increased release of presynaptic excitatory neurotransmitters²⁰. Clinical trials have shown that Gabapentin (GBP), a drug that binds to Cav $\alpha 2\delta 1$ ²⁵, is an effective treatment for neuropathic orofacial pain^{6, 48}. Therefore Cav $\alpha 2\delta 1$ might be a potential candidate for mediating the secondary hyperalgesia associated with trigeminal neuropathic pain.

Transient receptor potential ankyrin 1 (TRPA1) has been suggested to be a putative noxious cold sensor¹⁸ and to be involved in mechanosensation⁷, and thus it has been suggested to contribute to cold hyperalgesia and allodynia³². Channel silencing and pharmacological antagonism of TRPA1 in the peripheral nerves reduce the chemical, thermal, and mechanical hypersensitivity in different pain models^{3, 29}. It has also been proposed that expression of TRPA1 in the soma of trigeminal ganglion (TG) neurons mediates glyceryl trinitrate-induced pain in a migraine mouse model²⁶. Moreover, pain response behaviors in a model of trigeminal neuropathic pain are mediated by the TRPA1 channel⁴⁶. However, little is known of the role of TRPA1 in secondary

orofacial hyperalgesia.

Gap junctions (GJs) are composed of two hexameric connexins (Cxs) and are intercellular membrane channels that allow small molecules to pass directly between cells¹¹, which facilitates communication between neurons and glia cells^{38,42}. Protein expression of Cx26, Cx36, and Cx40 is increased in the TG following capsaicin or complete Freund's adjuvant injection into the temporomandibular joint¹⁰. Given that the nature of secondary hyperalgesia is the spreading of hypersensitivity from the injured area to the uninjured area, it is plausible that increased GJ coupling between neuronal or glial cells in the mouse TG plays a role in secondary orofacial hyperalgesia following peripheral injury.

Increased interaction of Cav α 2 δ 1 with thrombospondin-4 (TSP4) contributes to the pathogenesis of chronic pain following nerve injury through the activation of the downstream protein kinase C (PKC) signaling pathway¹². Additional evidence for a role for PKC in neuropathic pain comes from a report showing that GBP (the Cav α 2 δ 1 antagonist) inhibition of PKC signaling in the spinal cord of rats blocks such pain⁴⁹. PKC also has a putative role in enhancing TRPA1-mediated pain²⁴. Furthermore, activation of PKC modulates the phosphorylation, assembly, and thus the activity of GJs^{34,37}. In the present work, we examined the underlying role of Cav α 2 δ 1 expression and the activity of the downstream PKC-TRPA1 pathway and GJ signaling in trigeminal nerve injury-induced secondary hyperalgesia, especially cold hyperalgesia, in an orofacial neuropathic pain mouse model.

Materials and methods

Animals, surgery, and human tissues

The experiments were performed on adult male C57Bl/6 mice at 7~9 weeks of age. The mice were supplied by the Experimental Animal Center, Chinese Academy of Sciences, Shanghai, China. The mice were maintained under constant conditions (23 ± 0.5 °C and a 12:12 hour light/dark cycle) with food and water available ad libitum. Eight animals were housed per cage and allowed to acclimate to these conditions for at least 1 week before inclusion in the experiments. All animal procedures in this study were conducted in strict accordance with the National Institutes of Health Guide for the Care and Use of Laboratory Animals and the ethical standards of the International Association for the Study of Pain. All efforts were made to minimize both the number of animals used and their suffering. For each experiment, the animals were randomly divided into groups, and the sample size was calculated based on our previous work. The mice were subjected to peripheral neuropathy that was produced by partial transection of the infraorbital nerve (pT-ION). In brief, the oral cavity was exposed under anesthesia with sodium pentobarbital (50 mg/kg, intraperitoneally (i.p.)). Then an incision was made in the palatal-buccal mucosa to expose the ION. The deep branches of the ION that innervate the ventral part of the left vibrissal pad and the upper lip were tightly ligated with 4.0 catgut and sectioned distal to the ligation, removing 1–2 mm of the distal nerve stump (Fig 1A). Care was taken to avoid touching or stretching the ION. The incision was closed using tissue glue. For the sham surgeries, the ION was exposed as described above, but the nerve was not

ligated or cut. The human TGs from fixed postmortem tissue (two non-diseased donor corpses of a 60-year-old male and 54-year-old male) were kindly provided by the Fudan University body receiving station of the Shanghai Red Cross.

Mechanical hyperalgesia

Behavioral tests were conducted by experimenters blinded to the group allocation. To reduce any effects of restraint on the behavioral assessment of the mice, we adopted a less stressful method² to test mechanical hypersensitivity in the skin of the infraorbital area (V2) and the mandibular nerve area (V3). The mice were placed in a box (7 × 7 × 10 cms) made of black wire mesh and in which the mice were allowed to freely move. All mice were habituated to the box in a behavioral room for at least 30 min per day for 3 consecutive days prior to behavioral testing. To avoid head movement induced by tactile stimulation of the whisker hairs, the ipsilateral whisker hairs in the V2 and V3 measured region were removed. When the mouse's head was steady, a series of von Frey filaments (Stoelting, USA) were inserted through the mesh walls. The von Frey filaments had bending forces ranging from 0.07 g to 2.0 g and were applied to the skin between the border of the left whisker pad and the left eye within the V2 area and on the skin within the V3 area. Movement of the head away from the probing filament was defined as a positive response. Each von Frey filament was applied 5 times at intervals of a few seconds. The bending force (g) of the von Frey filament at which three positive responses were seen out of five stimulations was defined as the threshold. For the von Frey testing under red light in mice with intact whiskers, the mice were first habituated to stand on their hind paws

and to lean against the experimenter's hand wearing a regular cotton work glove in a quiet room under red light. The habituation required 0.5 h before the animals were tested with von Frey filaments on a region between the border of the left whisker pad and the left eye, carefully avoiding touching any whiskers.

Cold hypersensitivity

Cold hypersensitivity was assessed by measuring the response to acetone-evoked evaporative cooling. The mice were gently restrained, and a 50 μ l drop of 90% acetone (diluted in distilled water) was applied to the ipsilateral V3 skin by means of a customized 25-gauge needle (blunt and slightly bent) attached to a 1 ml syringe (Hamilton, Reno, NV), and care was taken to avoid any acetone getting in the eyes or nose. The nociceptive behavior evaluated in this study was rubbing and scratching the skin within the V3 area using the ipsilateral forepaw or hindpaw²². The total wiping time was recorded with an arbitrary maximum cutoff time of 2 min, and cold allodynia was assessed as increased rubbing and scratching after exposure to acetone compared to basal values and to sham-operated controls⁴⁶. Before testing, the mice were habituated to the experimental environment over a period of 2 to 3 consecutive days by taking a series of baseline measurements.

Rotarod test

To determine whether locomotor functions were altered in mice following GBP treatments, the rotarod test (ENV-575M, Med Associates, USA) was performed with saline or GBP (50 or 100 mg/kg i.p.)-treated mice. The drum was slowly accelerated from a speed of 4 rpm to 24 rpm over 180 seconds, and the length of time before

falling off the rotarod within this period was recorded by the Rotarod CUB software. The mice were habituated to the apparatus the day before testing by performing three unrecorded trials with a break of 30 min between each trial. The procedure was repeated on the testing day, and the mean time before falling off the rotarod was used for analysis.

Tissue immunofluorescence

The mice were deeply anesthetized with 1.5% sodium pentobarbital (50 mg/kg, i.p.) and then intracardially perfused with saline followed by 4% paraformaldehyde (PFA). The TG and trigeminal subnucleus caudalis (Vc) were removed, postfixed in 4% PFA for 12 hours, and allowed to equilibrate in 30% sucrose in a phosphate buffer for 5–7 days at 4 °C. The segments were embedded and frozen in encompassing agent (Leica, Germany) and then sectioned on a freezing microtome (Leica 2000, Germany) at a thickness of 8–10 µm for the TG and 30 µm for the Vc. After washing with PBST (phosphate-buffered saline with 0.3% Triton X-100) three times, the sections were blocked with 5% donkey serum for 1.5 h at room temperature and then incubated overnight at 4 °C with the following primary antibodies: mouse anti-Cav α 2 δ 1 antibody (1:100 dilution, sc-271697, Santa Cruz Biotechnology), rabbit anti-Cav α 2 δ 1 antibody (1:200 dilution, NBP1-86683, Novus), rabbit anti-NeuN antibody (1:500 dilution, ab177487, Abcam), goat anti-CGRP antibody (1:500 dilution, ab36001, Abcam), mouse anti-neurofilament 200 antibody (NF-200, 1:50 dilution, N5389, Sigma-Aldrich), rabbit anti-PKC α antibody (1:200 dilution, ab32376, Abcam), rabbit anti-phosphorylated PKC α antibody (phosphor S657+Y658, p-PKC α) (1:500 dilution,

ab23513, Abcam), goat anti-TRPA1 antibody (1:50 dilution, sc32356, Santa Cruz Biotechnology), mouse anti-Cx36 antibody (1:50 dilution, sc398063, Santa Cruz Biotechnology), mouse anti-Cx26 antibody (1:100 dilution, 13-8100, Thermo Fisher), and mouse anti-Cx43 antibody (1:100 dilution, 35-5000, Thermo Fisher). The sections were then washed with PBST three times and incubated with a mixture of Alexa 488-conjugated secondary antibodies, Alexa 594-conjugated secondary antibodies, and Alexa 647-conjugated IB4 antibodies (1:1,000 dilution, Invitrogen, USA) for 1.5 h at room temperature. All sections were washed three times and coverslipped with a mixture of 80% glycerin in 0.01 M PBS. Images were captured using a multiphoton laser point scanning confocal microscopy system (FV1000, Olympus, Tokyo, Japan). Relative immunofluorescence density was evaluated by using ImageJ (version 1.47). For immunohistochemistry of human TG samples, the procedure was the same as above but omitting the intracardial perfusion and adding antigen retrieval with the Quick Antigen Retrieval Solution for Frozen Sections kit (P0090, Beyotime, China).

Tissue immunohistochemistry

Immunohistochemistry staining was used to determine the location of Cav α 2 δ 1, TRPA1, PKC α , Cx26, Cx36, and Cx43 in the human TG tissue. The tissue specimens were embedded in paraffin and sliced into thin sections (5 μ m) after fixing in 4% formaldehyde. Xylene, an alcohol gradient, and distilled water were used for deparaffinization of the sections, followed by treatment with 3% H₂O₂ to block the endogenous peroxidase activity. Endogenous peroxidase blockage and heat-induced epitope retrieval were performed according to the manufacturer's protocol. The

expression of Cav α 2 δ 1, TRPA1, PKC α , Cx26, Cx36, and Cx43 was observed using an Olympus Cx31 microscope with the Image-Pro Plus medical image analysis system.

Tissue western blot

The mice were anesthetized with sodium pentobarbital (50 mg/kg, i.p.). The TG and Vc were quickly removed, and the V2 and V3 regions of the Vc (Vc-V2 and Vc-V3) were separately aspirated with a 50 ml syringe. The TG, Vc-V2, and Vc-V3 were ultrasonically disrupted in radioimmunoprecipitation assay (RIPA) lysis buffer (Beyotime, Shanghai, China), followed by centrifugation at 12,000 \times g. The total protein level in the supernatant was measured using the Pierce bicinchoninic acid (BCA) Protein Assay Kit (Thermo Scientific, Rockford, IL, USA). The protein samples were separated by 10% SDS-PAGE and then transferred onto polyvinylidene fluoride (PVDF) membranes (Millipore, Billerica, MA, USA). After blocking with 5% nonfat milk dissolved in 1% TBST (20 mM Tris-HCl, pH 7.5, 150 mM NaCl, and 0.05% Tween-20) for 1.5 h at room temperature, the membranes were probed with the following primary antibodies: mouse anti-Cav α 2 δ 1 antibody (1:1,000 dilution, sc-271697, Santa Cruz Biotechnology), HRP-conjugated mouse anti- β -actin antibody (1:10,000 dilution, 4967, Cell Signaling Technology), rabbit anti-phosphorylated PKC α antibody (phosphor S657+Y658, p-PKC α) (1:500 dilution, ab23513, Abcam), goat anti-TRPA1 antibody (1:50 dilution, sc32356, Santa Cruz Biotechnology), HRP-conjugated rabbit anti-GAPDH antibody (1:10,000 dilution, HRP-60004, Proteintech), mouse anti-Cx36 antibody (1:50 dilution, sc398063, Santa Cruz Biotechnology), mouse anti-Cx26 antibody (1:100 dilution, 13-8100, Thermo Fisher),

and mouse anti-Cx43 antibody (1:100 dilution, 35-5000, Thermo Fisher) at 4 °C overnight. The blots were washed in TBST and incubated with the following secondary antibodies: HRP-conjugated goat anti-mouse IgG (H+L) secondary antibody (1:10,000 dilution, SA00001-1, Proteintech), HRP-conjugated goat anti-rabbit IgG (H+L) secondary antibody (1:10,000 dilution, SA00001-2, Proteintech), and HRP-conjugated rabbit anti-goat IgG (H+L) secondary antibody (1:10,000 dilution, SA00001-4, Proteintech) for 1–2 h at room temperature. Western blot images were captured on an ImageQuant LAS4000 mini image analyzer (GE Healthcare, Buckinghamshire, UK), and band intensities were quantified using the Quantity One analysis software (Version 4.6.2, Bio-Rad Laboratories, Hercules, USA). The protein band densities were normalized against the density of β -actin or GAPDH. The fold change of the control group was set as 1 for quantifications.

Drug administration

In order to determine the role of Cav α 2 δ 1 in pT-ION-induced trigeminal neuropathic pain, the Cav α 2 δ 1 inhibitor GBP (ab120219, Abcam) was delivered i.p. using a 1 ml syringe. In order to block the function of PKC, TRPA1, and GJs, the PKC inhibitor GF109203X (GFX, Selleck, USA), the selective TRPA1 inhibitor HC030031 (Selleck, USA), and the GJ inhibitor carbenoxolone (CBX) (a special GJ blocker, ab143590, Abcam) were administered i.p. The administration time and dosage were determined by preliminary experiments.

Adeno-associated virus 2/6 (AAV2/6) preparation and injection

Cav α 2 δ 1-specific short hairpin RNA (shRNA) was packaged as an AAV2/6 virus

(pAOV-SYN-MCS-EGFP-3FLAG-alpha2deltal micro30 shRNA) by OBIO Technology Co., Ltd. (Shanghai, China). The AAV-scrambled shRNA-EGFP was used as the control. The human synapsin promoter was chosen because it has previously been shown to result in neuron-specific transduction^{44, 45}. For the Cav α 2 δ 1 overexpression experiment, the full-length coding sequence of mouse Cav α 2 δ 1 (NM_001110843) in the AAV2/6 vector was designed and purchased from OBIO Technology Co., Ltd. For virus injection, mice were anesthetized with 1.5% sodium pentobarbital (50 mg/kg, i.p.). After disinfecting with alternating applications of ethanol and betadine solution, 6 μ l of virus used for overexpressing (Ove) Cav α 2 δ 1 (AAV-Cav α 2 δ 1-Ove virus) was injected subcutaneously at three points (2 μ l/point) in the V2 area (the skin within the infraorbital territory and the whisker pad) of naïve mice, and 6 μ l of virus used for interfering (Int) (AAV-Cav α 2 δ 1-Int virus) was injected subcutaneously at three points in the V3 area (lower jaw and pre-auricular area) of pT-ION mice at 1 μ l/min using a 10 μ l syringe (Hamilton Company). Care was taken to minimize damage to the injection site as much as possible. The dose of AAV-Cav α 2 δ 1-Int virus in the subcutaneous delivery was 1.27×10^{13} viral genome (v.g.)/ml, and the dose of AAV-Cav α 2 δ 1-Ove virus was 2.14×10^{13} v.g./ml.

Experiments in the SH-SY5Y cell line

Cell line and culture

Human SH-SY5Y cells were obtained from the Shanghai Institute of Cell Biology, Chinese Academy of Sciences (Shanghai, China). The cells were cultured in DMEM supplemented with 10% fetal bovine serum, 2 mmol/L glutamine (Gibco, Grand

Island, NY, USA), penicillin (100 U/mL), and streptomycin (100 µg/mL) and maintained at 37 °C and 5% CO₂ in a humidified environment. The culture medium was replaced twice each week.

Transfection of short hairpin RNA (shRNA) and overexpression RNA

SH-SY5Y cells (2×10^5) were seeded onto a culture dish with a diameter of 10 cm. Transfection of shRNA was performed using Lipofectamine 3000 (Invitrogen, USA) according to the manufacturer's instructions. The Cav α 2 δ 1-specific shRNAs (Y3779: GCA ATG AAG TTG TCT ACT A; Y3780: GCA TGC AGC GGT CCA TAT T; and Y3781: GCC AAA GCC TAT TGG TGT A) and the Cav α 2 δ 1 overexpression RNA (NM_001110843) were purchased from OBIO Technology Co., Ltd. Thirty-six hours after shRNA or overexpression RNA transfection, the transfection efficiency was determined using an ordinary fluorescence microscope (Olympus, Japan).

Immunohistochemistry staining

For immunohistochemistry, SH-SY5Y cells were fixed with 4% PFA for 30 min and permeabilized with 0.2% Triton X-100 for 15 min at room temperature and processed as described previously⁴³. Cell preparations were incubated with the following primary antibodies: mouse anti-Cav α 2 δ 1 antibody (1:100 dilution, sc-271697, Santa Cruz Biotechnology), rabbit anti-phosphorylated PKC α antibody (phosphor S657+Y658, p-PKC α) (1:500 dilution, ab23513, Abcam), and goat anti-TRPA1 antibody (1:50 dilution, sc32356, Santa Cruz Biotechnology). The sections were then washed with PBST three times and incubated with a mixture of Alexa 488-conjugated secondary antibodies or Alexa 594-conjugated secondary antibodies. All signals were

analyzed with a multiphoton laser point scanning confocal microscopy system (FV1000, Olympus, Tokyo, Japan).

Western blotting

After being collected by centrifugation, the SH-SY5Y cells were suspended in ice-cold lysis buffer and homogenized. The homogenates were centrifuged at $10,000 \times g$ at $4\text{ }^{\circ}\text{C}$ for 10 min to obtain the supernatants and the pellets, and the protein concentrations were determined using the Bio-Rad protein assay kit. Equal protein amounts were electrophoresed on 10% SDS gels and transferred to PVDF membranes. Membranes were blocked with 5% nonfat milk dissolved in 1% TBST for 1.5 h at room temperature, then incubated overnight at $4\text{ }^{\circ}\text{C}$ with the following primary antibodies: mouse anti-Cav α 2 δ 1 antibody (1:1,000 dilution, sc-271697, Santa Cruz Biotechnology), HRP-conjugated mouse anti- β -actin antibody (1:10,000 dilution, 4967, Cell Signaling Technology), rabbit anti-phosphorylated PKC α antibody (phosphor S657+Y658, p-PKC α) (1:500 dilution, ab23513, Abcam), goat anti-TRPA1 antibody (1:50 dilution, sc32356, Santa Cruz Biotechnology), and HRP-conjugated rabbit anti-GAPDH antibody (1:10,000 dilution, HRP-60004, Proteintech). The immunoblot membranes were then incubated with the HRP-conjugated goat anti-mouse IgG (H+L) secondary antibody (1:10,000 dilution, SA00001-1, Proteintech), the HRP-conjugated goat anti-rabbit IgG (H+L) secondary antibody (1:10,000 dilution, SA00001-2, Proteintech), and the HRP-conjugated rabbit anti-goat IgG (H+L) secondary antibody (1:10,000 dilution, SA00001-4, Proteintech) for 1–2 h at room temperature. The immunoreactive proteins were visualized on an ImageQuant

LAS4000 mini image analyzer (GE Healthcare). Densitometry was performed with the Quantity One analysis software (Version 4.6.2, Bio-Rad Laboratories).

Quantitative PCR (qPCR) analysis

Total RNA was extracted from the TG and Vc tissues using Trizol-chloroform (Sigma) and then treated with DNase I (Invitrogen). The cDNA was prepared using the Prime Script RT reagent Kit (Takara). Quantitative PCR was performed using the Takara SYBR Green reagents on an Applied Biosystems 7300 plus according to the manufacturer's protocol. The thermal cycling conditions were as follows: 1 cycle at 95 °C for 30 s followed by 40 cycles at 95 °C for 5 s and 60 °C for 34 s. The primers were mouse Cav α 2 δ 1 forward, GCA GCC AAC GGA TTA AAC CTG and mouse Cav α 2 δ 1 reverse, CGT GGG AAT ATG GAC CGC T. Relative mRNA levels were calculated using the $2^{-\Delta\Delta CT}$ method and normalized to the *Gapdh* level in the same sample.

Statistical analysis

The animal data are shown as the mean \pm SEM (standard error of the mean). All statistical analyses were performed in GraphPad Prism 6 (GraphPad Software Inc., San Diego, CA, USA). The statistical significance of differences between groups was analyzed with Student's t-test or one-way analysis of variance (ANOVA) followed by a Dunnett multiple comparison test or Tukey's test. Analysis of the time course of mechanical and cold hyperalgesia was performed using two-way repeated-measures ANOVA followed by a Tukey's test or Sidak's test. Pearson's correlation was used for the linear correlation analysis. $p < 0.05$ was used as the threshold of significance in all

analyses.

Results

Trigeminal nerve injury induced up-regulation of the Cava2δ1 subunit proteins that correlated with orofacial hyperalgesia and the therapeutic effects of gabapentin.

The trigeminal nerve can be divided into the ophthalmic (V1), maxillary (V2), and mandibular (V3) areas ³³, and we previously reported that CCI-ION mice exhibit long-lasting mechanical hyperalgesia in areas innervated by injured and uninjured nerves ³⁶. In this work, we developed the pT-ION model of neuropathic pain in mice (Fig 1A). Consistent with the CCI-ION model, the pT-ION model exhibits both primary hyperalgesia and secondary hyperalgesia. Mechanical hyperalgesia was measured as reductions compared to baseline in the response threshold to mechanical stimuli using von Frey filaments. The ipsilateral orofacial V2 response thresholds of the pT-ION mice were significantly decreased from the 3rd day after surgery, and the effect was stable from the 7th day and lasted for at least 28 days after surgery (two-way ANOVA and Tukey's test, $F_{2,21} = 786.7$, $p < 0.0001$, Fig 1B), while the V3 nociceptive threshold was also decreased over the same time frame (two-way ANOVA and Tukey's test, $F_{2,21} = 999.3$, $p < 0.0001$, Fig 1C). It should be noted that the decrease in thresholds in the V3 area was a little bit smaller compared with the V2 area at 3 days after surgery, indicating a trend of delayed occurrence of secondary hyperalgesia compared with primary hyperalgesia. In addition to the presence of long-lasting mechanical hyperalgesia in both the V2 and V3 areas, cold hyperalgesia

in the V3 area was also elicited using the acetone test. Compared with the sham group and baseline, the pT-ION mice had a significantly longer duration of wiping on the orofacial V3 area than that recorded in sham mice starting from 3 days and persisting for up to 28 days after surgery (two-way ANOVA and Tukey's test, $F_{2,21} = 294.6$, $p < 0.0001$, Fig 1D), indicating the occurrence of secondary cold hyperalgesia in the pT-ION model. Because of the difficulty in avoiding acetone being sprayed into the eyes, we did not test primary cold hyperalgesia by administering acetone to the V2 area. We obtained similar results when performing the von Frey testing under red light in mice with intact whiskers (Fig S1).

To confirm that Cava2 δ 1 plays a role in mediating neuropathic orofacial pain, we injected GBP, a drug that binds to the Cava2 δ 1 protein and has anti-allodynia properties, into pT-ION mice with established hyperalgesia on the 15th day after surgery to determine whether it could reverse pT-ION-induced hyperalgesia. Bolus i.p. injection of 5 mg/kg GBP resulted in a small and statistically insignificant attenuation of pT-ION-induced hyperalgesia. However, increasing the GBP dose to 50 and 100 mg/kg resulted in a significant attenuation of injury-induced orofacial hyperalgesia (two-way ANOVA and Tukey's test, von Frey Test-V2: $F_{4,35} = 702.1$, $p < 0.0001$; von Frey Test-V3, $F_{4,35} = 1214$, $p < 0.0001$, Fig 1E,F) from 0.5 h to 8 h, and these effects peaked at 4 h after administration. Unlike saline, the i.p. administration of GBP attenuated the development of cold hyperalgesia in the pT-ION mice (two-way ANOVA and Tukey's test, $F_{4,35} = 73.72$, $P < 0.0001$, Fig 1G). In contrast, no significant effect of GBP was observed in sham mice (Fig S2). To test whether GBP

treatment impaired locomotor functions, rotarod tests were performed before and 4 h after i.p. GBP injection, which was the time point that correlated with maximal attenuation of orofacial hyperalgesia in GBP-treated pT-ION mice. We found that 100 mg/kg GBP impaired the motor performance of the mice, while 50 mg/kg showed no significant impairment in motor performance (one-way ANOVA and Dunnett's test, $F = 7.727$, $p < 0.0001$; pT-ION+GBP (100 mg/kg) vs. pT-ION+saline: $p = 0.0006$; pT-ION+GBP (50 mg/kg) vs. pT-ION+saline: $p = 0.9717$; Fig 1H). These data suggest that Cav α 2 δ 1 is highly likely to be involved in primary and secondary hyperalgesia processing in the pT-ION mouse model.

If pT-ION induces the Cav α 2 δ 1 dysregulation that plays a role in orofacial pain, there should be a correlation between changes in Cav α 2 δ 1 expression in the TG and/or Vc and the development of orofacial hyperalgesia. To test this hypothesis, we examined the expression level of Cav α 2 δ 1 in the TG, Vc-V2, and Vc-V3 at different stages of orofacial hyperalgesia development. Our results showed that the expression of Cav α 2 δ 1 was significantly increased by the 3rd day after pT-ION and was maintained at high levels until the final examination on the 28th day in the TG (one-way ANOVA and Dunnett's test, $F = 5.099$, $p = 0.0017$) and Vc-V2 (one-way ANOVA and Dunnett's test, $F = 13.98$, $p < 0.0001$) (Fig 2E, F). This was negatively correlated with the orofacial response threshold (g) observed in the V2 area (Linear regression analysis, TG-Cav α 2 δ 1: $R^2 = 0.7671$, $Y = -0.7948 * X + 2.23$, $p < 0.0001$; Vc-V2-Cav α 2 δ 1: $R^2 = 0.7243$, $Y = -2.268 * X + 4.735$, $p < 0.0001$; Fig 2H). In Vc-V3, the expression of Cav α 2 δ 1 was increased by the 5th day, peaked on the 14th

day, and was maintained at high levels until the final examination on the 28th day (one-way ANOVA and Dunnett's test, $F = 7.006$, $p = 0.0002$; Fig 2G). Cav α 2 δ 1 expression in the TG and Vc-V3 was negatively correlated with the orofacial response threshold (g) observed in the V3 area (TG-Cav α 2 δ 1: $R^2 = 0.6902$, $Y = -0.7566 * X + 2.295$, $p < 0.0001$; Vc-V3-Cav α 2 δ 1: $R^2 = 0.6144$, $Y = -0.6393 * X + 2.007$, $p = 0.0001$; Fig 2I) and positively correlated with duration of wiping (s) in the V3 area (TG-Cav α 2 δ 1: $R^2 = 0.6529$, $Y = 0.1715 * X + 0.0608$, $p < 0.0001$; Vc-V3-Cav α 2 δ 1: $R^2 = 0.6018$, $Y = 0.1438 * X + 0.0275$, $p = 0.0002$; Fig 2J). This correlation between injury-induced Cav α 2 δ 1 up-regulation and hyperalgesia suggests that increased Cav α 2 δ 1 might play a critical role in the induction of primary and secondary orofacial processing. It should be noted that Cav α 2 δ 1 mRNA expression was increased only in TG but not in Vc samples (Fig 2A,B,C,D), indicating a potential specific presynaptic up-regulation of Cav α 2 δ 1.

To determine the location of Cav α 2 δ 1 expression in the TG in response to injury-induced orofacial pain, we measured the Cav α 2 δ 1 immunoreactivity in TG samples from the injury side from pT-ION mice. Confocal microscopy of immunofluorescent staining showed Cav α 2 δ 1 expression in small, medium, and large-size TG neurons (Fig S3D). To further characterize the neurochemical properties of Cav α 2 δ 1-positive neurons, we performed staining for Cav α 2 δ 1 along with staining for CGRP, a marker of peptidergic C-nociceptors; IB4, a marker of nonpeptidergic C-nociceptors; and NF200, a marker of A-fiber afferents. Cav α 2 δ 1 was colocalized with all three markers in TG-V2 and TG-V3 (Fig S3A,B,C), suggesting that Cav α 2 δ 1

is expressed in TG neurons with different neurochemical properties.

The expression of p-PKC and TRPA1 in the TG and Vc was increased after nerve injury.

TRPA1 has been suggested to be a putative noxious cold sensor¹⁸ involved in mechanosensation⁷ and contributing to cold hyperalgesia and allodynia³². Previous studies reported that GBP binds to Cav α 2 δ 1 and modulates PKC signaling in the spinal cord dorsal horn^{49,52}. PKC is involved in the regulation of pain by modulating the thermo-sensitive transient receptor potential (TRP) channels, including TRPA1²⁴, and among all of the isoforms of PKC, the PKC α -dependent ERK1/2 signaling pathway has been reported to contribute to neuronal hyperexcitability in TG neurons⁵¹. To test whether PKC-TRPA1 signaling mediates primary and secondary orofacial hyperalgesia downstream of Cav α 2 δ 1 activation after nerve injury, we determined the distribution and expression of phosphorylated PKC α (p-PKC α), the active form of PKC α , and TRPA1 in the V2 and V3 areas of both TG and Vc samples in sham and pT-ION mice. Double staining results showed that p-PKC α and TRPA1 were colocalized with Cav α 2 δ 1 in both the V2 and V3 areas of the TG (Fig 3A,B,C) and Vc (mostly expressed in superficial layers, Fig 3G,H). pT-ION induced a significant increase in the expression of p-PKC and TRPA1 in the TG (one-way ANOVA and Dunnett's test, TG-p-PKC: $F = 14.66$, $p = 0.0001$; TG-TRPA1: $F = 17.2$, $p < 0.0001$; Fig 3D,E,F), Vc-V2 (one-way ANOVA and Dunnett's test, V2-p-PKC: $F = 16.74$, $p < 0.0001$; V2-TRPA1: $F = 18.97$, $p < 0.0001$; Fig 3I,J,K), and Vc-V3 (one-way ANOVA and Dunnett's test, V3-p-PKC: $F = 6.886$, $p = 0.004$; V3-TRPA1: $F = 9.542$, $p = 0.001$;

Fig 3L,M,N) from the 7th day after surgery and throughout the 28 days of observation. The expression levels of p-PKC and TRPA1 were positively correlated with the expression of Cav α 2 δ 1 in the TG (TG-p-PKC: $R^2 = 0.2585$, $Y = 1.251 * X + 0.2008$, $p = 0.0221$; TG-TRPA1: $R^2 = 0.4481$, $Y = 0.944 * X + 0.1627$, $p = 0.0012$; Fig 3O), Vc-V2 (V2-p-PKC: $R^2 = 0.4019$, $Y = 0.5245 * X + 0.8101$, $p = 0.0027$; V2-p-PKC: $R^2 = 0.5557$, $Y = 0.5976 * X + 0.7375$, $p = 0.0002$; Fig 3P), and Vc-V3 (V3-p-PKC: $R^2 = 0.2131$, $Y = 0.8646 * X + 0.5999$, $p = 0.0405$; V3-p-PKC: $R^2 = 0.2676$, $Y = 0.7239 * X + 0.9904$, $p = 0.0211$; Fig 3Q).

Subcutaneous treatment with Cav α 2 δ 1 shRNA in AAV2/6 vectors in the V3 skin area in pT-ION mice reversed secondary hyperalgesia and up-regulated p-PKC-TRPA1 protein levels in the TG and Vc-V3.

To further determine whether pT-ION-induced Cav α 2 δ 1 up-regulation plays a critical role in mediating secondary hyperalgesia and whether PKC-TRPA1 signaling serves as the downstream signaling pathway, we administered a single injection of Cav α 2 δ 1 shRNA or control shRNA in the AAV2/6 virus vector subcutaneously at three sites (2 μ l/site, 1.27×10^{13} v.g./ml) within the V3 region of the skin (the antero-ear and lower jaw) on the 7th day after pT-ION when the injured mice had developed stable hyperalgesia in order to determine whether knock-down of Cav α 2 δ 1 could block or diminish pT-ION-induced secondary hyperalgesia by decreasing downstream PKC-TRPA1 levels. Because there is still some debate as to whether GBP might target other molecules than Cav α 2 δ 1¹, we used shRNA packaged in the AAV virus to specifically down-regulate the expression of Cav α 2 δ 1. Briefly, three plasmids (Y3779,

Y3780, and Y3781) were designed and transfected into SH-SY5Y cells, and the proteins in the SH-SY5Y cells were extracted when the transfection efficiency reached 60%. Western blot results showed that all three plasmids successfully down-regulated the expression of Cav α 2 δ 1, with Y3781 showing the most significant knock-down effects (Fig S4). Using SYN as a promoter of mature neurons, the Y3781 plasmid was packaged into the AAV2/6 vector, which specifically transfects mature neurons. The affect of transfection was tested in SH-SY5Y cells and shown to be significant (Fig S6B-C). To down-regulate the expression of Cav α 2 δ 1 in the TG-V3 specifically, the virus was injected into the facial V3 area (Fig 4A). The von Frey test and cold allodynia test were performed at 14 days and 21 days after the virus injection. Here we developed a method that allowed us to explore the mechanisms of primary and secondary hyperalgesia separately by specifically targeting protein expression in the TG-V2 or TG-V3 by subcutaneously injecting virus through the V2 or V3 skin, respectively. The AAV2/6 viral vector can traffic from the nerve terminal in the skin of the whisker pad in a retrograde manner, reach the neuronal body, and specifically transfect these neurons without affecting the adjacent neurons⁴⁴. A strong EGFP signal from the virus was observed only in the Vc-V3 area 21 days after virus injection (Fig 4B, Fig S5). As indicated in Fig 4F,G,H, subcutaneous treatments with the interfering, but not control, virus resulted in a time-dependent attenuation of secondary hyperalgesia (von Frey Test-V2: two-way ANOVA and Sidak's test, pT-ION+AAV-Cav α 2 δ 1-Int virus vs. pT-ION+AAV-control virus, $F_{1,16} = 0.2011$, $p = 0.6598$; von Frey Test-V3: two-way ANOVA and Sidak's test, pT-ION+

AAV-Cav α 2 δ 1-Int virus vs. pT-ION+AAV-control virus, $F_{1,16} = 18.65$, $p = 0.0005$; Acetone Test-V3: two-way ANOVA and Sidak's test, pT-ION+ AAV-Cav α 2 δ 1-Int virus vs. pT-ION+AAV-control virus, $F_{1,16} = 43.15$, $p < 0.0001$). The interfering effects had an onset time of 14 days after treatment initiation (i.e. 21 days after nerve injury) and lasted throughout the whole observation period (i.e. 21–28 days after nerve injury). In contrast, the injection of AAV-Cav α 2 δ 1-Int virus did not affect the pain thresholds in naïve mice (Fig S7). To determine whether the knock-down effects were due to blockade of pT-ION-induced up-regulation of Cav α 2 δ 1 and the potential downstream PKC-TRPA1 signaling, we examined Cav α 2 δ 1 and PKC-TRPA1 protein levels in dorsal Vc-V3 and TG samples collected from pT-ION mice 21 days after the initial treatment with Cav α 2 δ 1 interfering or control virus. Data from western blot analyses indicated that treatments with interfering virus, but not with control virus, caused statistically significant reversal of the injury-induced increase of Cav α 2 δ 1 and PKC-TRPA1 in both the TG and Vc-V3 (Fig 4C,D). The expression change in Cav α 2 δ 1 and PKC-TRPA1 showed a positive correlation (TG-p-PKC: $R^2 = 0.6619$, $Y = 1.052 * X + 0.1777$, $p = 0.0013$; TG-TRPA1: $R^2 = 0.7931$, $Y = 0.8708 * X + 0.1133$, $p = 0.0001$; Vc-V3-p-PKC: $R^2 = 0.6801$, $Y = 1.036 * X + 0.1282$, $p = 0.001$; Vc-V3-TRPA1: $R^2 = 0.8431$, $Y = 1.098 * X - 0.0337$, $p < 0.0001$; Fig 4E), indicating that PKC-TRPA1 possibly acts downstream of Cav α 2 δ 1. This correlation in interfering virus-mediated blockade between injury-induced secondary hyperalgesia and Cav α 2 δ 1 and PKC-TRPA1 up-regulation supports the hypothesis that pT-ION-induced Cav α 2 δ 1 and PKC-TRPA1 up-regulation in the TG and Vc-V3 plays

a critical role in the development of secondary hyperalgesia.

Cava2δ1 overexpression in TG-V2 neurons induced primary and secondary hyperalgesia and up-regulated Cav2δ1 and p-PKC-TRPA1 proteins in the TG, Vc-V2, and Vc-V3.

Changes in Cavα2δ1 expression can lead to changes in calcium channel current density and thus can affect the normal processing of sensory information. However, nerve injury might also result in altered expression of other genes and proteins that might also contribute to the development of chronic neuropathic pain. Thus, the causal link between the Cavα2δ1 up-regulation induced by pT-ION and neuropathic pain remains unclear. To determine whether increased expression of Cavα2δ1 is sufficient to mediate abnormal sensations associated with the induction of primary and secondary hyperalgesia and whether PKC-TRPA1 is the downstream signaling pathway, we specifically overexpressed Cavα2δ1 in TG-V2 neurons. To study the relationship between Cavα2δ1 and PKC-TRPA1, we first determined whether Cavα2δ1 overexpression in TG-V2 neurons increased PKC-TRPA1 expression. Briefly, the H6856 plasmid was designed and transfected into SH-SY5Y cells, and the proteins in the SH-SY5Y cells were extracted when the transfection efficiency reached 60%. Western blot results showed that the H6856 plasmid successfully overexpressed Cavα2δ1 (Fig S8). SYN was used as a promoter of mature neurons, and the H6856 plasmid was packaged into AAV2/6, which specifically transfects mature neurons. We used subcutaneous injection of AAV-Cavα2δ1-Ove virus into the whisker pad V2 area (at three sites, 2 μl/site, 2.14×10^{13} v.g./ml, Fig 5A), which

effectively induced transgene expression in TG-V2 neurons. Transfection with AAV-Cav α 2 δ 1-Ove virus significantly increased Cav α 2 δ 1 protein levels and the expression of PKC-TRPA1 in the TG, Vc-V2, and Vc-V3 (Fig 5B,C). The results from SH-SY5Y cells were consistent with this finding (Fig S9). Cav α 2 δ 1 overexpression in TG-V2 neurons caused mechanical and cold hyperalgesia in the whisker pad V2 and V3 areas from 14 days after virus injection, whereas injection of AAV-control virus had no effect (two-way ANOVA and Tukey's test, von Frey Test-V2: $F_{3,28} = 16.73$, $p < 0.0001$; von Frey Test-V3: $F_{3,28} = 11.32$, $p < 0.0001$; Acetone Test-V3: $F_{3,28} = 10.94$, $p < 0.0001$; Fig 5D,E,F). The pain hypersensitivity induced by Cav α 2 δ 1 overexpression was readily reversed by systemic injection of HC03001, a specific TRPA1 antagonist, at 1 h after injection (Naïve+AAV-Cav α 2 δ 1-Ove virus vs. Naïve+AAV-Cav α 2 δ 1-Ove virus +HC03001, two-way ANOVA and Sidak's test, von Frey Test-V2: $F_{1,14} = 2.505$, $p = 0.1358$, 1h - $p = 0.0434$; von Frey Test-V3: $F_{1,14} = 2.451$, $p = 0.1398$, 1h - $p = 0.0325$; Acetone Test-V3: $F_{1,14} = 1.046$, $p = 0.3238$, 1h - $p = 0.0391$; Fig 5D,E,F).

GJ expression was upregulated in the TG in response to nerve injury.

Consistent with our previous reports^{17,33}, the current study found that nerve injury induced hyperalgesia outside of the injury area, i.e. secondary hyperalgesia. However, the mechanisms of secondary hyperalgesia remain obscure. Our previous work found that the serotonergic descending facilitation from the rostral ventromedial medulla contributes to the maintenance of secondary hyperalgesia in a mouse CCI-ION model¹⁷. In the present study, secondary hyperalgesia was detected at a very early stage, i.e.

from the 3rd day after nerve injury, almost simultaneously with the primary hyperalgesia. Cav α 2 δ 1 overexpression in TG-V2 neurons could mimic the above effect. Therefore, we conclude that in the very periphery, there should be rapid activation of TG-V3 neurons by TG-V2 neurons through a Cav α 2 δ 1-associated pathway. Cx26 and Cx36 have been shown to be increased in the TG following capsaicin or complete Freund's adjuvant injection into the temporomandibular joint ¹⁰, and Cx43 has been shown to be increased in the TG following CCI-ION surgery ²². Therefore GJs might be potential candidates for the rapid activation between adjacent neurons within the TG, and so we first examined the expression and distribution of Cx26, Cx36, and Cx43 in sham and pT-ION mice. Antibodies directed against the three Cxs were used to determine their cellular expression and localization in the TG obtained from sham animals and from animals with nerve injury known to cause primary and secondary hyperalgesia. Based on the immunohistochemistry and western blot data, Cx26, Cx36, and Cx43 were well colocalized with Cav α 2 δ 1 (Fig 6A,B,C), and the expression of all three Cxs was significantly increased starting from the 7th day after nerve injury (one-way ANOVA and Dunnett's test, TG-Cx26: $F = 7.32$, $p = 0.0032$; TG-Cx36: $F = 8.569$, $p = 0.0017$; TG-Cx43: $F = 6.595$, $p = 0.0048$; Fig 6D,E,F,G). The expression of Cxs was positively correlated with the expression of Cav α 2 δ 1 in the TG (TG-Cx26: $R^2 = 0.3630$, $Y = 0.6365 * X + 0.5297$, $p = 0.0049$; TG-Cx36: $R^2 = 0.2122$, $Y = 1.295 * X + 0.3026$, $p = 0.0409$; TG-Cx43: $R^2 = 0.3448$, $Y = 0.8541 * X + 0.2680$, $p = 0.0065$; Fig 6H)

Cava2 δ 1 overexpression in TG-V2 neurons up-regulated Cx26, Cx36, Cx43 in the

TG and induced hyperalgesia that was inhibited by the GJ blocker carbenoxolone.

To determine whether GJs are involved in rapid activation of TG-V3 neurons by TG-V2 neurons, we first determined whether Cav α 2 δ 1 overexpression in TG-V2 neurons increased GJ expression. Transfection with AAV-Cav α 2 δ 1-Ove virus significantly increased Cav α 2 δ 1 protein levels and the expression of Cx26, Cx36, and Cx43 in the TG, Vc-V2, and Vc-V3 (Fig 7A,B,C). The mechanical hypersensitivity induced by Cav α 2 δ 1 overexpression was reversed by systemic injection of CBX (100 mg/kg), a specific GJ blocker, starting from 0.5 h up to 2 h after injection (two-way ANOVA with Tukey's test, von Frey Test-V2: $F_{3,28} = 36.81$, $p < 0.0001$; von Frey Test-V3: $F_{3,28} = 29.59$, $p < 0.0001$; Fig 7D,E). In addition, CBX also significantly reversed the cold allodynia in the whisker pad V3 area only at the testing point at 0.5 h after injection (Acetone Test-V3: $F_{3,28} = 11.57$, $p < 0.0001$; Fig 7F).

Nerve injury and Cava2 δ 1 overexpression in TG-V2 neurons up-regulated TRPA1, Cx26, Cx36, and Cx43 in the TG/Vc and induced hyperalgesia that was inhibited by the PKC inhibitor GFX.

To further determine whether PKC acts downstream of Cav α 2 δ 1 and upstream of TRPA1 and GJs in the development of primary and secondary hyperalgesia, we tested the effects of PKC blockade on hyperalgesic behavior and the expression of TRPA1 and GJs. At 14 days after pT-ION, the systemic administration of the PKC inhibitor GFX (0.2 mg/kg) significantly reversed mechanical hypersensitivity induced by nerve injury starting from 0.5 h up to 4 h (V2) and 6 h (V3) after injection (two-way ANOVA with Tukey's test, von Frey Test-V2: $F_{4,36} = 313.1$, $p < 0.0001$; von Frey

Test-V3: $F_{4,36} = 222.9$, $p < 0.0001$; Fig 8A,B). GFX also significantly reversed the cold allodynia in the whisker pad V3 area only at the testing point at 1 h after injection (Acetone Test-V3: $F_{4,36} = 23.86$, $p < 0.0001$; Fig 8C). At 21 days after surgery, the systemic administration of the PKC inhibitor GFX transiently reversed mechanical hypersensitivity induced by Cav α 2 δ 1 overexpression at 0.5 h and 1 h (V2 and V3) after injection (two-way ANOVA with Tukey's test, von Frey Test-V2: $F_{3,28} = 18.98$, $p < 0.0001$; von Frey Test-V3: $F_{3,28} = 16.50$, $p < 0.0001$; Fig 8D,E). GFX also significantly reversed the cold allodynia in the whisker pad V3 area only at the testing point at 1 h after injection (Acetone Test-V3: $F_{3,28} = 6.183$, $p = 0.0023$; Fig 8F). The increase in the expression of TRPA1, Cx26, Cx36, and Cx43 in the TG (Fig 8G), Vc-V2 (Fig 8H), and Vc-V3 (Fig 8I) was significantly reversed by the PKC inhibitor GFX.

Cav α 2 δ 1, PKC-TRPA1, Cx26, Cx36, and Cx43 are expressed in the human TG.

Finally, we checked the expression of Cav α 2 δ 1, PKC-TRPA1, Cx26, Cx36, and Cx43 in the TG from fixed postmortem human tissues. Immunohistochemistry data showed that Cav α 2 δ 1, PKC α -TRPA1, Cx26, Cx36, and Cx43 were expressed in the human TG (Fig 9A,B). Moreover, PKC α , TRPA1, NF-200, CGRP, and IB4 were colocalized with Cav α 2 δ 1 (Fig 9B,C). These results suggest the possible involvement of Cav α 2 δ 1 signaling in human pain conditions.

Discussion

There are very few effective treatments for orofacial neuropathic pain, and development of therapeutic interventions has been limited due to a poor understanding

of the underlying mechanisms behind the etiology of such pain. The main findings of this study are that injury to the secondary branch of the trigeminal nerve leads to up-regulation of Cav α 2 δ 1 in the TG and the dorsal Vc-V3 area that correlates with the mechanical and cold hyperalgesia in the whisker pad V3 area, both of which could be blocked by specifically knocking down Cav α 2 δ 1 expression in TG-V3 neurons. The mechanical and cold hyperalgesia were attenuated by GBP, a drug that binds to Cav α 2 δ 1²⁵. In addition, pT-ION induced the upregulation of PKC-TRPA1/GJ proteins (Cx26, Cx36, and Cx43) in the TG, Vc-V2, and Vc-V3 that correlated with the increased expression of Cav α 2 δ 1 and mechanical and cold hyperalgesia in the injured and uninjured area, which could be mimicked by the overexpression of Cav α 2 δ 1 in TG-V2 neurons. Moreover, both the TRPA1 antagonist and the GJ blocker significantly reversed the secondary mechanical and cold hyperalgesia as well as the primary mechanical hyperalgesia. Together, these findings support the hypothesis that Cav α 2 δ 1 up-regulation induced by trigeminal nerve injury mediates secondary mechanical and cold orofacial hypersensitivity through a mechanism involving PKC-TRPA1/GJ signaling (Fig 9D).

We used a mouse model of pT-ION to produce constant and long-lasting primary hyperalgesia in the V2 area and secondary hyperalgesia in areas innervated by the mandibular branch. Selectively targeting TG-V3 neurons by subcutaneous AAV2/6 injection through the whisker pad V3 area provided a useful tool to investigate the underlying mechanisms of primary and secondary hyperalgesia separately. We tested cold allodynia using acetone applied onto the facial skin of the V3 area following

pT-ION in the mice, and the results were consistent with a previous report²¹. Also, the mice used in the present study exhibited pain-related behaviors that were consistent with the pain that occurs in patients with trigeminal neuralgia¹⁹. Cold allodynia is a common symptom in patients with trigeminal neuropathic pain and spinal cord injury³⁹. In the present study, rAAV2/6 transduced to TG-V3 neurons after subcutaneous delivery. Further optimization of subcutaneous delivery of rAAV2/6, might make it an alternative to herpes simplex virus in human gene therapy for pain, and rAAV is currently the only viral vector being studied in clinical trials for neurological disease.

Gabapentinoids, including GBP and pregabalin, bind to Cav α 2 δ 1 and are widely used in the treatment of neuropathic pain and epilepsy⁹. However, although gabapentinoids have been used clinically for several decades, the molecular mechanisms behind their therapeutic effects are poorly understood. In addition, studies on the effects of gabapentinoids on VGCCs have come to different conclusions. For example, chronic treatment with GBP has been shown to reduce VGCC activity in dorsal root ganglion neurons¹⁴, but other studies have reported that GBP has no effect on VGCC-mediated neurotransmitter release or on VGCC trafficking in cultured neurons^{4,15}. The present study found that the effects of GBP only lasted a few hours, indicating the inhibition of the function but not the expression of Cav α 2 δ 1 by GBP, which is consistent with previous work reporting that GBP showed analgesic effects even when the upregulation of Cav α 2 δ 1 expression was absent¹, and this might be why GBP impairs Cav α 2 δ 1 expression but does not seem to have any effect on VGCC currents. The inconsistent effects of GBP on VGCCs

might also be due to the weak interaction between Cav α 2 δ 1 and VGCC α 1 subunits²⁷.

It should also be noted that the expression of both Cav α 2 δ 1 mRNA and protein were increased in TGs, whereas only the expression of Cav α 2 δ 1 protein but not mRNA was increased in Vc, which indicates that the increased protein of Cav α 2 δ 1 in Vc comes from the presynaptic terminals due to increased synthesis in the cell bodies of TG neurons but not Vc neurons.

GBP has been reported to regulate PKC signaling in the spinal cord of rats in a model of neuropathic pain⁴⁹. Increased expression of TSP4 might therefore contribute to the pathogenesis of chronic pain following nerve injury by disrupting intracellular calcium signaling through its interaction with Cav α 2 δ 1 and subsequent activation of the PKC signaling pathway. In addition, Pan et al. recently reported that Cav α 2 δ 1 interacts with NMDARs⁵. Therefore, Cav α 2 δ 1 might act as a scaffold protein by interacting with both TSP4 and NMDARs. According to the above, pT-ION induces increased binding of Cav α 2 δ 1 to either TSP4 or NMDA receptors, which upon activation will increase the amount of Ca²⁺ entering the neurons and thus activate PKC and the downstream signaling molecules.

The function or expression of TRPA1 might be directly or indirectly modulated by PKC^{24, 28, 31}, the downstream effector of Cav α 2 δ 1. The present study indicates that upregulation of TRPA1 in the TG and Vc-V3 plays an important role in the development of secondary mechanical and cold hyperalgesia. In terms of how TRPA1 was upregulated and activated in TG-V3, one possibility is that an unidentified mechanism is activated within the injured V2 nerve trunk and neurons leading to the

activation of neighboring TG-V3 neurons, which subsequently causes the upregulation and activation of TRPA1. In the present study, PKC was found to be simultaneously upregulated together with TRPA1, indicating TRPA1 as a possible downstream of PKC. TRPA1 has been suggested to be a putative noxious cold sensor¹⁸ that is involved in mechanosensation⁷ and contributes to cold hyperalgesia or allodynia³². Therefore, it is reasonable that blockade of TRPA1 by an antagonist could alleviate the secondary mechanical and cold hyperalgesia detected in the whisker pad V3 area. The SH-SY5Y cell line maintains many properties of nerve cells, providing a useful model for investigating the characterization of endogenously expressed Cav α 2 δ 1 channels³⁵. In the present study, the upregulation of PKC-TRPA1 induced by Cav α 2 δ 1 overexpression was confirmed in SH-SY5Y cells.

It should be noted that Cav α 2 δ 1 was expressed in most TG neurons of different sizes, predominantly in small (< 20 μ m) and medium (20–40 μ m) neurons after nerve injury (Fig S3) in mice. Meanwhile, nerve injury increased the number of Cav α 2 δ 1-immunoreactive profiles over 25 μ m in diameter with a trend of more pronounced increases in larger diameter profiles in a rat CCI-ION model²⁰. However PKC and TRPA1 only locate in a subset of TG neurons, and TRPA1 and TRPV1 are usually considered to be co-localized in nociception-specific neurons. Therefore, the Cav α 2 δ 1-PKC-TRPA1 signaling pathway might underlie the role of nociception-specific neurons in pain-related behavior. Given that Cav α 2 δ 1 is a subunit of all subtypes of VGCCs (including T-type, L-type, etc.), the downstream pathway might be versatile. The influx of Ca²⁺ subsequent to the activation of VGCCs

might activate many kinds of Ca^{2+} -dependent kinases, such as CaMK II, PKA, etc., other than PKC. In a rat model, CCI-ION leads to abnormal excitatory synapse formation²⁰, which is always the result of CaMK II activation. Therefore, it is possible that other Ca^{2+} -dependent kinases and pathways might contribute to the development of secondary hyperalgesia.

GJs are the other target besides TRPA1 modulated by PKC, the downstream effector of $\text{Cav}\alpha 2\delta 1$ ³⁴. Dong and colleagues¹⁶ provided direct evidence for electrical coupling between neurons and between neurons and SGCs, and they discovered that adjacent neurons tend to be activated together following injury. Such activation of coupled neurons thus represents a novel mechanism behind mechanical or cold hyperalgesia and allodynia⁸. The TG expresses several kinds of Cxs, including Cx26 located between neurons, Cx36 located between neurons and SGCs, and Cx43 located between SGCs¹⁰. We found in the present study that secondary mechanical and cold hyperalgesia developed very early, on the 3rd day after pT-ION, almost simultaneously with primary hyperalgesia. Therefore it is reasonable to assume that rapid activation of TG-V3 neurons by TG-V2 neurons through GJs underlies the rapid initiation of hyperalgesia in the V3 area. Hyperalgesia outside the site of injury, which in this case was hyperalgesia in the skin of the V3 area, is common in chronic pain conditions and is thought to be related to activity within the central nervous system³⁶. The present work proposes a potential GJ-mediated peripheral mechanism. We found that the expression of GJ proteins was upregulated after $\text{Cav}\alpha 2\delta 1$ overexpression and that CBX significantly alleviated the $\text{Cav}\alpha 2\delta 1$ overexpression-induced secondary

hyperalgesia. It is possible that GJs in the TG mediate the activation of TG-V3 neurons by the initial injured nerve; however, the action of central GJs cannot be excluded due to the ability of CBX to cross the blood brain barrier.

In conclusion, our results support the hypothesis that pT-ION leads to up-regulation of Cav α 2 δ 1 in the TG and Vc and that this contributes to the development of secondary orofacial neuropathic pain through the PKC-TRPA1/GJ signaling pathway. The mechanisms presented here suggest potential targets for drug development, and TRPA1 or GJ blockade might prove useful in clinical practice. Future studies should investigate new cofactors of this pathway alone or in combination with GBP in terms of their therapeutic benefits for the management of chronic orofacial neuropathic pain.

Funding sources

This study was financially supported by the National Natural Science Funds of China (31600852, 81473749, 81771202, 81873101), the National Key R&D Program of China (2017YFB0403803), and the Development Project of Shanghai Peak Disciplines-Integrated Medicine (20180101).

Author contributions

YX.C. and WQ.C. designed the experiments and wrote the paper; WQ.C., YX.C., F.X., and T.C. carried out most of the experiments and image analysis; L.G., Y.F., XM.H., W.Y., LX.D., and WW.Z. performed the experiments; QL.MY., WL.M., and YQ.W. provided valuable advice on the research; All authors discussed the results and the manuscript.

Declarations of interest

The authors declare that there is no conflict of interest regarding the publication of this paper.

Data and materials availability

The data that support the findings of this study are available from the corresponding author on reasonable request.

References

1. Abe M, Kurihara T, Han W, Shinomiya K, Tanabe T: Changes in expression of voltage-dependent ion channel subunits in dorsal root ganglia of rats with radicular injury and pain. *Spine (Phila Pa 1976)* 27:1517-1524, 1525, 2002
2. Aita M, Byers MR, Chavkin C, Xu M: Trigeminal injury causes kappa opioid-dependent allodynic, glial and immune cell responses in mice. *Mol Pain* 6:8, 2010
3. Andrade EL, Meotti FC, Calixto JB: TRPA1 antagonists as potential analgesic drugs. *Pharmacol Ther* 133:189-204, 2012
4. Cassidy JS, Ferron L, Kadurin I, Pratt WS, Dolphin AC: Functional exofacially tagged N-type calcium channels elucidate the interaction with auxiliary alpha2delta-1 subunits. *Proc Natl Acad Sci U S A* 111:8979-8984, 2014
5. Chen J, Li L, Chen SR, Chen H, Xie JD, Sirrieh RE, MacLean DM, Zhang Y, Zhou MH, Jayaraman V, Pan HL: The alpha2delta-1-NMDA Receptor Complex Is Critically Involved in Neuropathic Pain Development and Gabapentin Therapeutic Actions. *Cell Rep* 22:2307-2321, 2018
6. Clark GT: Persistent orodental pain, atypical odontalgia, and phantom tooth pain: when are they

neuropathic disorders? *J Calif Dent Assoc* 34:599-609, 2006

7. Corey DP, Garcia-Anoveros J, Holt JR, Kwan KY, Lin SY, Vollrath MA, Amalfitano A, Cheung EL, Derfler BH, Duggan A, Géléoc GS, Gray PA, Hoffman MP, Rehm HL, Tamasauskas D, Zhang DS: TRPA1 is a candidate for the mechanosensitive transduction channel of vertebrate hair cells. *Nature* 432:723-730, 2004

8. Devor M, Wall PD: Cross-excitation in dorsal root ganglia of nerve-injured and intact rats. *J Neurophysiol* 64:1733-1746, 1990

9. Dworkin RH, O'Connor AB, Audette J, Baron R, Gourlay GK, Haanpaa ML, Kent JL, Krane EJ, Lebel AA, Levy RM, Mackey SC, Mayer J, Miaskowski C, Raja SN, Rice AS, Schmader KE, Stacey B, Stanos S, Treede RD, Turk DC, Walco GA, Wells CD: Recommendations for the pharmacological management of neuropathic pain: an overview and literature update. *Mayo Clin Proc* 85:S3-S14, 2010

10. Garrett FG, Durham PL: Differential expression of connexins in trigeminal ganglion neurons and satellite glial cells in response to chronic or acute joint inflammation. *Neuron Glia Biol* 4:295-306, 2008

11. Goldberg GS, Moreno AP, Lampe PD: Gap junctions between cells expressing connexin 43 or 32 show inverse permselectivity to adenosine and ATP. *J Biol Chem* 277:36725-36730, 2002

12. Guo Y, Zhang Z, Wu HE, Luo ZD, Hogan QH, Pan B: Increased thrombospondin-4 after nerve injury mediates disruption of intracellular calcium signaling in primary sensory neurons. *Neuropharmacology* 117:292-304, 2017

13. Gurnett CA, De Waard M, Campbell KP: Dual function of the voltage-dependent Ca²⁺ channel alpha 2 delta subunit in current stimulation and subunit interaction. *Neuron* 16:431-440,

1996

14. Hendrich J, Van Minh AT, Heblich F, Nieto-Rostro M, Watschinger K, Striessnig J, Wratten J, Davies A, Dolphin AC: Pharmacological disruption of calcium channel trafficking by the alpha2delta ligand gabapentin. *Proc Natl Acad Sci U S A* 105:3628-3633, 2008
15. Hoppa MB, Lana B, Margas W, Dolphin AC, Ryan TA: alpha2delta expression sets presynaptic calcium channel abundance and release probability. *Nature* 486:122-125, 2012
16. Kim YS, Anderson M, Park K, Zheng Q, Agarwal A, Gong C, Saijilafu, Young L, He S, LaVinka PC, Zhou F, Bergles D, Hanani M, Guan Y, Spray DC, Dong X: Coupled Activation of Primary Sensory Neurons Contributes to Chronic Pain. *Neuron* 91: 1085-1096, 2016.
17. Kim YS, Chu Y, Han L, Li M, Li Z, LaVinka PC, Sun S, Tang Z, Park K, Caterina MJ, Ren K, Dubner R, Wei F, Dong X: Central terminal sensitization of TRPV1 by descending serotonergic facilitation modulates chronic pain. *Neuron* 81:873-887, 2014
18. Kwan KY, Allchorne AJ, Vollrath MA, Christensen AP, Zhang DS, Woolf CJ, Corey DP: TRPA1 contributes to cold, mechanical, and chemical nociception but is not essential for hair-cell transduction. *Neuron* 50:277-289, 2006
19. Lemos L, Fontes R, Flores S, Oliveira P, Almeida A: Effectiveness of the association between carbamazepine and peripheral analgesic block with ropivacaine for the treatment of trigeminal neuralgia. *J Pain Res* 3:201-212, 2010
20. Li KW, Yu YP, Zhou C, Kim DS, Lin B, Sharp K, Steward O, Luo ZD: Calcium channel alpha2delta1 proteins mediate trigeminal neuropathic pain states associated with aberrant excitatory synaptogenesis. *J Biol Chem* 289:7025-7037, 2014
21. Lim EJ, Jeon HJ, Yang GY, Lee MK, Ju JS, Han SR, Ahn DK: Intracisternal administration of

mitogen-activated protein kinase inhibitors reduced mechanical allodynia following chronic constriction injury of infraorbital nerve in rats. *Prog Neuropsychopharmacol Biol Psychiatry* 31:1322-1329, 2007

22. Luccarini P, Childeric A, Gaydier AM, Voisin D, Dallel R: The orofacial formalin test in the mouse: a behavioral model for studying physiology and modulation of trigeminal nociception. *J Pain* 7:908-914, 2006

23. Luo ZD, Calcutt NA, Higuera ES, Valder CR, Song YH, Svensson CI, Myers RR: Injury type-specific calcium channel alpha 2 delta-1 subunit up-regulation in rat neuropathic pain models correlates with antiallodynic effects of gabapentin. *J Pharmacol Exp Ther* 303:1199-1205, 2002

24. Mandadi S, Armati PJ, Roufogalis BD: Protein kinase C modulation of thermo-sensitive transient receptor potential channels: Implications for pain signaling. *J Nat Sci Biol Med* 2:13-25, 2011

25. Marais E, Klugbauer N, Hofmann F: Calcium channel alpha (2)delta subunits-structure and Gabapentin binding. *Mol Pharmacol* 59:1243-1248, 2001

26. Marone IM, De Logu F, Nassini R, De Carvalho GM, Benemei S, Ferreira J, Jain P, Li Puma S, Bunnnett NW, Geppetti P, Materazzi S: TRPA1/NOX in the soma of trigeminal ganglion neurons mediates migraine-related pain of glyceryl trinitrate in mice. *Brain* 141:2312-2328, 2018

27. Muller CS, Haupt A, Bildl W, Schindler J, Knaus HG, Meissner M, Rammner B, Striessnig J, Flockerzi V, Fakler B, Schulte U: Quantitative proteomics of the Cav2 channel nano-environments in the mammalian brain. *Proc Natl Acad Sci U S A* 107:14950-14957, 2010

28. Munro FE, Fleetwood-Walker SM, Mitchell R: Evidence for a role of protein kinase C in the sustained activation of rat dorsal horn neurons evoked by cutaneous mustard oil application.

Neurosci Lett 170:199-202, 1994

29. Nassini R, Materazzi S, Benemei S, Geppetti P: The TRPA1 channel in inflammatory and neuropathic pain and migraine. *Rev Physiol Biochem Pharmacol* 167:1-43, 2014

30. Newton RA, Bingham S, Case PC, Sanger GJ, Lawson SN: Dorsal root ganglion neurons show increased expression of the calcium channel α 2delta-1 subunit following partial sciatic nerve injury. *Brain Res Mol Brain Res* 95:1-8, 2001

31. Nilius B, Owsianik G, Voets T, Peters JA: Transient receptor potential cation channels in disease. *Physiol Rev* 87:165-217, 2007

32. Obata K, Katsura H, Mizushima T, Yamanaka H, Kobayashi K, Dai Y, Fukuoka T, Tokunaga A, Tominaga M, Noguchi K: TRPA1 induced in sensory neurons contributes to cold hyperalgesia after inflammation and nerve injury. *J Clin Invest* 115:2393-2401, 2005

33. Okubo M, Castro A, Guo W, Zou S, Ren K, Wei F, Keller A, Dubner R: Transition to persistent orofacial pain after nerve injury involves supraspinal serotonin mechanisms. *J Neurosci* 33:5152-5161, 2013

34. Pahujaa M, Anikin M, Goldberg GS: Phosphorylation of connexin43 induced by Src: regulation of gap junctional communication between transformed cells. *Exp Cell Res* 313:4083-4090, 2007

35. Reeve HL, Vaughan PF, Peers C: Calcium channel currents in undifferentiated human neuroblastoma (SH-SY5Y) cells: actions and possible interactions of dihydropyridines and omega-conotoxin. *Eur J Neurosci* 6:943-952, 1994

36. Ringkamp M, Meyer RA: Injured versus uninjured afferents: Who is to blame for neuropathic pain? *Anesthesiology* 103:221-223, 2005

37. Rong B, Xie F, Sun T, Hao L, Lin MJ, Zhong JQ: Nitric oxide, PKC-epsilon, and connexin43 are crucial for ischemic preconditioning-induced chemical gap junction uncoupling. *Oncotarget* 7:69243-69255, 2016
38. Rouach N, Avignone E, Meme W, Koulakoff A, Venance L, Blomstrand F, Giaume C: Gap junctions and connexin expression in the normal and pathological central nervous system. *Biol Cell* 94:457-475, 2002
39. Scrivani S, Wallin D, Moulton EA, Cole S, Wasan AD, Lockerman L, Bajwa Z, Upadhyay J, Becerra L, Borsook D: A fMRI evaluation of lamotrigine for the treatment of trigeminal neuropathic pain: pilot study. *Pain Med* 11:920-941, 2010
40. Shibuta K, Suzuki I, Shinoda M, Tsuboi Y, Honda K, Shimizu N, Sessle BJ, Iwata K: Organization of hyperactive microglial cells in trigeminal spinal subnucleus caudalis and upper cervical spinal cord associated with orofacial neuropathic pain. *Brain Res* 1451:74-86, 2012
41. Smith JG, Elias LA, Yilmaz Z, Barker S, Shah K, Shah S, Renton T: The psychosocial and affective burden of posttraumatic neuropathy following injuries to the trigeminal nerve. *J Orofac Pain* 27:293-303, 2013
42. Spataro LE, Sloane EM, Milligan ED, Wieseler-Frank J, Schoeniger D, Jekich BM, Barrientos RM, Maier SF, Watkins LR: Spinal gap junctions: potential involvement in pain facilitation. *J Pain* 5:392-405, 2004
43. Tanaka Y, Engelender S, Igarashi S, Rao RK, Wanner T, Tanzi RE, Sawa A, Dawson V, Dawson TM, Ross CA: Inducible expression of mutant alpha-synuclein decreases proteasome activity and increases sensitivity to mitochondria-dependent apoptosis. *Hum Mol Genet* 10:919-926, 2001

44. Towne C, Pertin M, Beggah AT, Aebischer P, Decosterd I: Recombinant adeno-associated virus serotype 6 (rAAV2/6)-mediated gene transfer to nociceptive neurons through different routes of delivery. *Mol Pain* 5:52, 2009
45. Towne C, Raoul C, Schneider BL, Aebischer P: Systemic AAV6 delivery mediating RNA interference against SOD1: neuromuscular transduction does not alter disease progression in fALS mice. *Mol Ther* 16:1018-1025, 2008
46. Trevisan G, Benemei S, Materazzi S, De Logu F, De Siena G, Fusi C, Fortes Rossato M, Coppi E, Marone IM, Ferreira J, Geppetti P, Nassini R: TRPA1 mediates trigeminal neuropathic pain in mice downstream of monocytes/macrophages and oxidative stress. *Brain* 139:1361-1377, 2016
47. Tsuboi Y, Takeda M, Tanimoto T, Ikeda M, Matsumoto S, Kitagawa J, Teramoto K, Simizu K, Yamazaki Y, Shima A, Ren K, Iwata K: Alteration of the second branch of the trigeminal nerve activity following inferior alveolar nerve transection in rats. *Pain* 111:323-334, 2004
48. Vickers ER, Cousins MJ: Neuropathic orofacial pain. Part 2-Diagnostic procedures, treatment guidelines and case reports. *Aust Endod J* 26:53-63, 2000
49. Yeh CY, Chung SC, Tseng FL, Tsai YC, Liu YC: Biphasic effects of chronic intrathecal gabapentin administration on the expression of protein kinase C gamma in the spinal cord of neuropathic pain rats. *Acta Anaesthesiol Taiwan* 49:144-148, 2011
50. Zakrzewska JM, Wu J, Mon-Williams M, Phillips N, Pavitt SH: Evaluating the impact of trigeminal neuralgia. *Pain* 158:1166-1174, 2017
51. Zhang Y, Wang H, Ke J, Wei Y, Ji H, Qian Z, Liu L, Tao J: Inhibition of A-Type K⁺ Channels by Urotensin-II Induces Sensory Neuronal Hyperexcitability Through the PKCalpha-ERK

Pathway. *Endocrinology* 159:2253-2263, 2018

52. Zhang YB, Guo ZD, Li MY, Fong P, Zhang JG, Zhang CW, Gong KR, Yang MF, Niu JZ, Ji

XM, Lv GW: Gabapentin Effects on PKC-ERK1/2 Signaling in the Spinal Cord of Rats with

Formalin-Induced Visceral Inflammatory Pain. *Plos One* 10:e141142, 2015

Figures legends

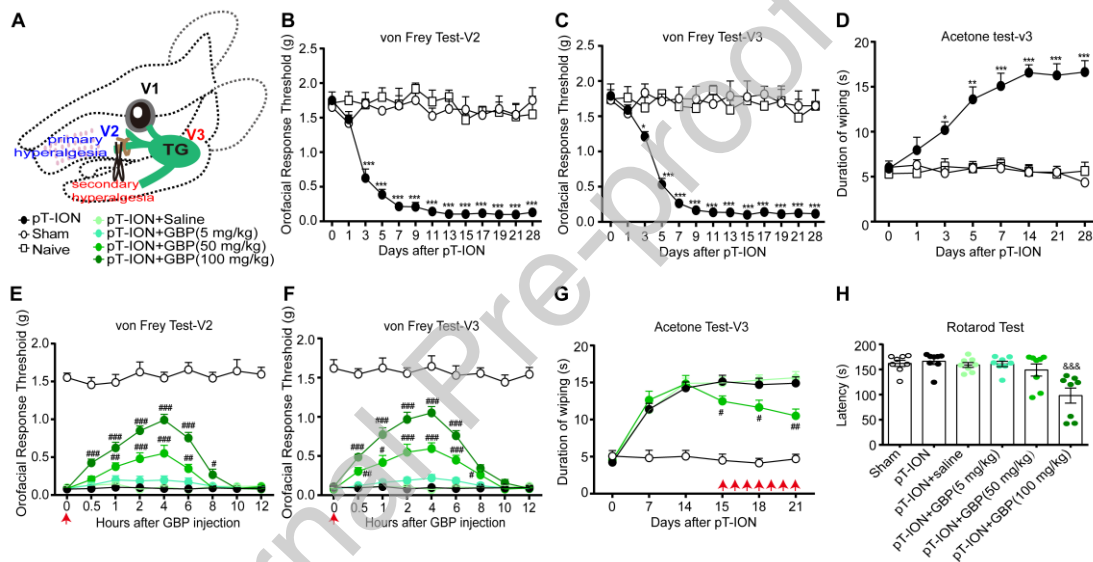


Figure 1. The time course of primary and secondary hyperalgesia after nerve injury

and the therapeutic effect of intraperitoneal injection of gabapentin. The schematic

diagram of pT-ION and orofacial nerve innervation in the trigeminal system (**A**).

pT-ION induced long-lasting primary hyperalgesia in the ipsilateral V2 skin (**B**) and

secondary hyperalgesia in the ipsilateral V3 skin (**C**) as shown by reduced thresholds

to mechanical stimuli. Secondary cold hyperalgesia was also induced in the V3 skin

as shown by increased duration of wiping in response to acetone stimulation (**D**).

Intraperitoneal (*i.p.*) injection of gabapentin at the doses indicated suppressed both

primary (E) and secondary (F) mechanical hyperalgesia. Behavioral testing was performed on the injury side before the injection of gabapentin and at the indicated time points after the injection. Effects of i.p. administration of gabapentin on cold hyperalgesia elicited by pT-ION (G). Rotarod tests showed that the high dose of gabapentin (100 mg/kg) decreased the latency to fall in the rotarod test (H). Rotarod tests were performed before and 4 h after intraperitoneal gabapentin injection, the time point that correlated with the maximal attenuation of orofacial hyperalgesia in GBP-treated pT-ION mice. Data presented are the means \pm SEM, n = 8 mice for each group, * $p < 0.05$, ** $p < 0.01$, *** $p < 0.001$ compared with the sham group, # $p < 0.05$, ## $p < 0.01$, ### $p < 0.001$ compared with the pT-ION group, &&& $p < 0.001$ compared with the pT-ION+saline group. The red arrows indicate the GBP treatment time points. The behavioral data were analyzed by two-way ANOVA with Tukey's test. The rotarod test data were analyzed by one-way ANOVA with Dunnett's test.

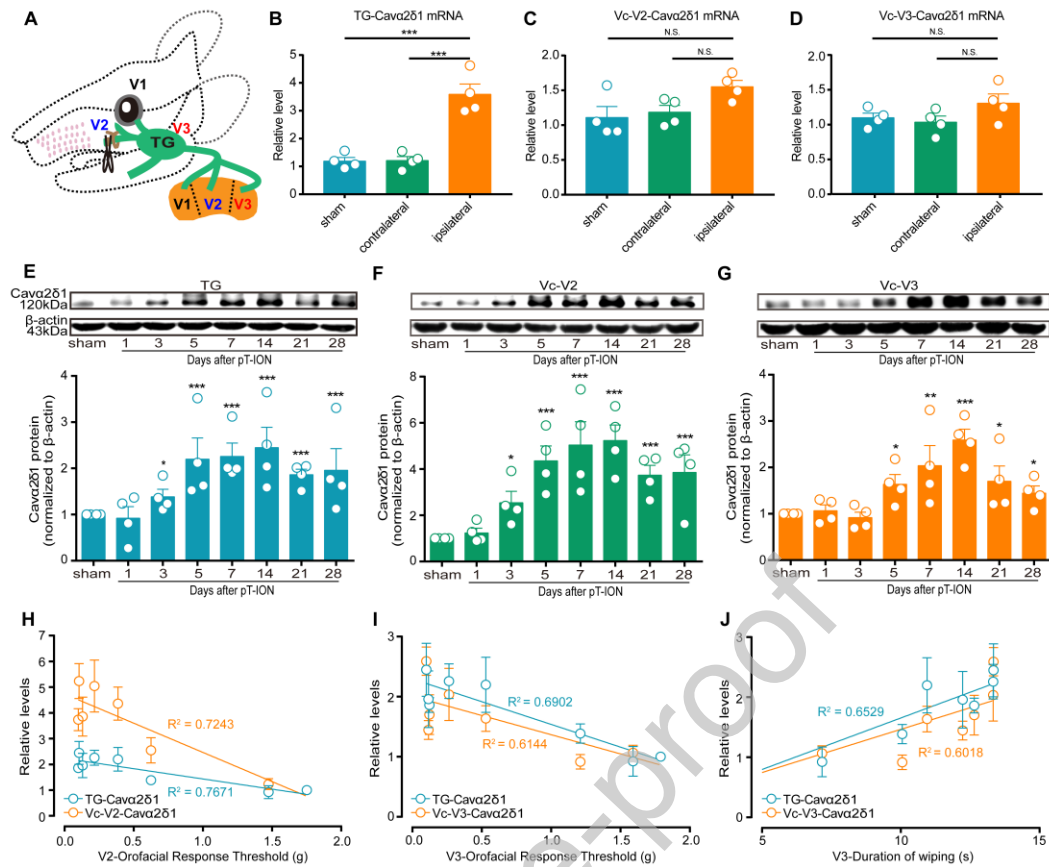


Figure 2. Expression of Cavα2δ1 in the TG and Vc after nerve injury. The anatomy of the orofacial and trigeminal system is shown (A). The Cavα2δ1 mRNA expression in the ipsilateral TG, Vc-V2, and Vc/V3 from sham (n = 4) and pT-ION mice (n = 4) at day 14 after surgery (B-D); *** $p < 0.001$ compared with the sham group according to one-way ANOVA analysis. The time course of Cavα2δ1 expression after pT-ION in the TG, Vc-V2, and Vc-V3 (the Cavα2δ1 expression in sham group was evaluated at day 14 after surgery) (E-G); n = 4 mice for each group, * $p < 0.05$; ** $p < 0.01$, *** $p < 0.001$ compared with sham group according to one-way ANOVA analysis. There was a linear correlation between the expression of Cavα2δ1 and the orofacial response threshold (g) observed in the V2 area (H, TG-Cavα2δ1: $R^2 = 0.7671$, $p < 0.0001$; Vc-V2-Cavα2δ1: $R^2 = 0.7243$, $p < 0.0001$) and V3 area (I, TG-Cavα2δ1: $R^2 = 0.6902$, $p < 0.0001$; Vc-V3-Cavα2δ1: $R^2 = 0.6144$, $p = 0.0001$). There was also a linear

correlation between the expression of Cav α 2 δ 1 and duration of wiping (s) in the V3 area (**J**, TG-Cav α 2 δ 1: $R^2 = 0.6529$, $p < 0.0001$; Vc-V3-Cav α 2 δ 1: $R^2 = 0.6018$, $p = 0.0002$).

Journal Pre-proof

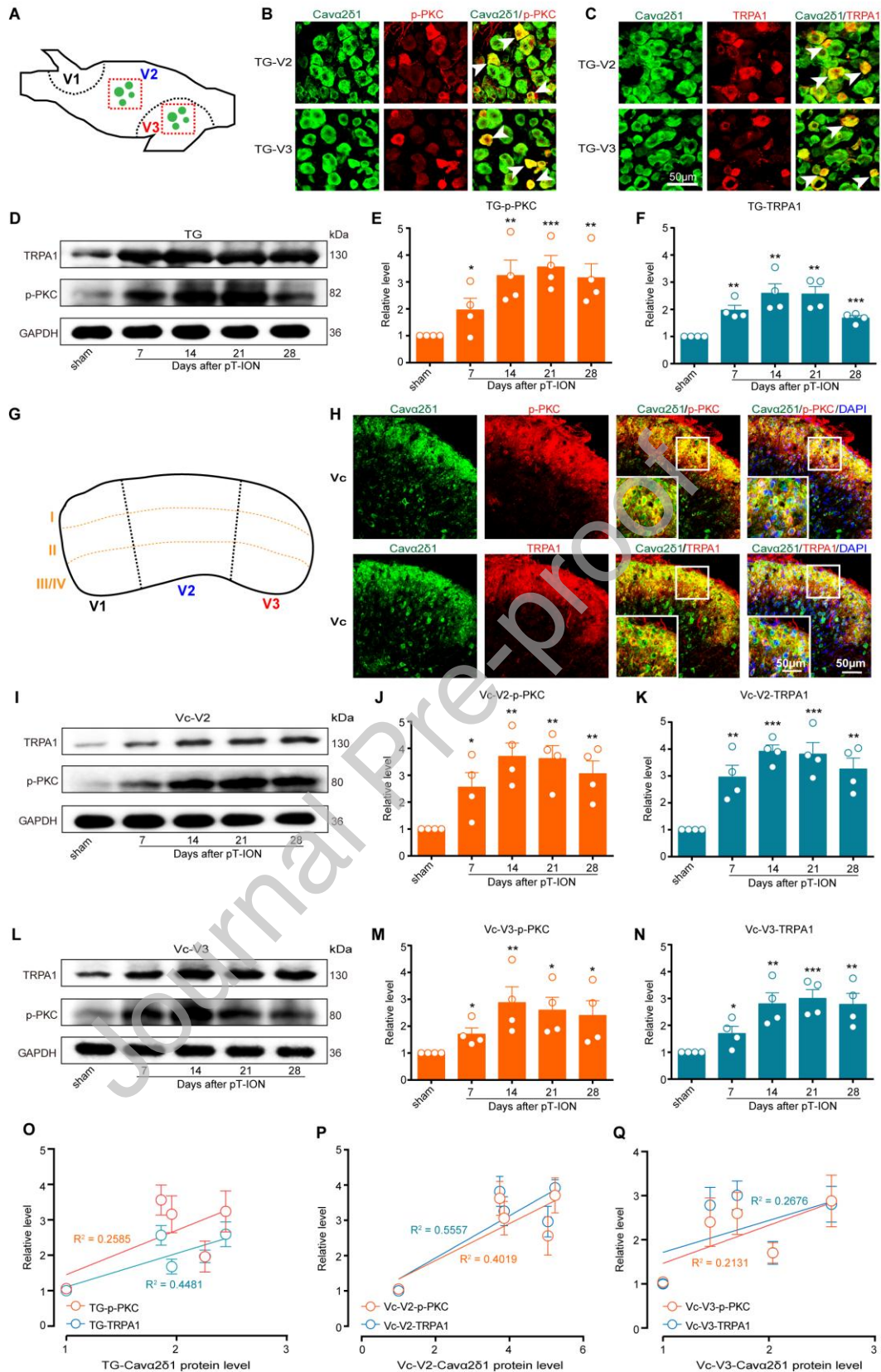


Figure 3. The up-regulated expression and distribution of p-PKC and TRPA1 in the TG and Vc after nerve injury. Schematic diagram of the three divisions of the mouse

TG (A). The black dashed lines indicate the borders of the three large divisions (V1, V2, and V3) in the TG. The red square boxes indicate where the images in B and C were taken. The colocalization of Cav α 2 δ 1 (green) with p-PKC (red) (B) and TRPA1 (red) (C) in the TG samples is shown. Scale bar: 50 μ m. pT-ION increased p-PKC and TRPA1 expression in the ipsilateral TG, and representative blots show the time course of p-PKC and TRPA1 protein expression in the TG (D). The histograms show the quantitative results (E and F). Schematic diagram showing the three divisions of the mouse Vc. The I, II, III/IV refer to different layers of the mouse Vc (G). The colocalization of Cav α 2 δ 1 (green) with p-PKC (red) and TRPA1 (red) in the Vc samples is shown (H). Scale bar: 50 μ m. Western blots show the significantly increased expression of p-PKC and TRPA1 in both Vc-V2 (I) and Vc-V3 (L) from 7 days after pT-ION. The histograms show the quantitative results (J, K, M, and N). Protein loading was normalized to the expression of GAPDH. * $p < 0.05$, ** $p < 0.01$, *** $p < 0.001$ compared with the sham group according to one-way ANOVA analysis, $n = 4$ mice for each group. The linear correlation between the expression of Cav α 2 δ 1 and the expression of p-PKC and TRPA1 in the TG (O, TG-p-PKC: $R^2 = 0.2585$, $p = 0.0221$; TG-TRPA1: $R^2 = 0.4481$, $p = 0.0012$), Vc-V2 (P, V2-p-PKC: $R^2 = 0.4019$, $p = 0.0027$; V2-TRPA1: $R^2 = 0.5557$, $p = 0.0002$), and Vc-V3 (Q, V3-p-PKC: $R^2 = 0.2131$, $p = 0.0405$; V3-TRPA1: $R^2 = 0.2676$, $p = 0.0211$).

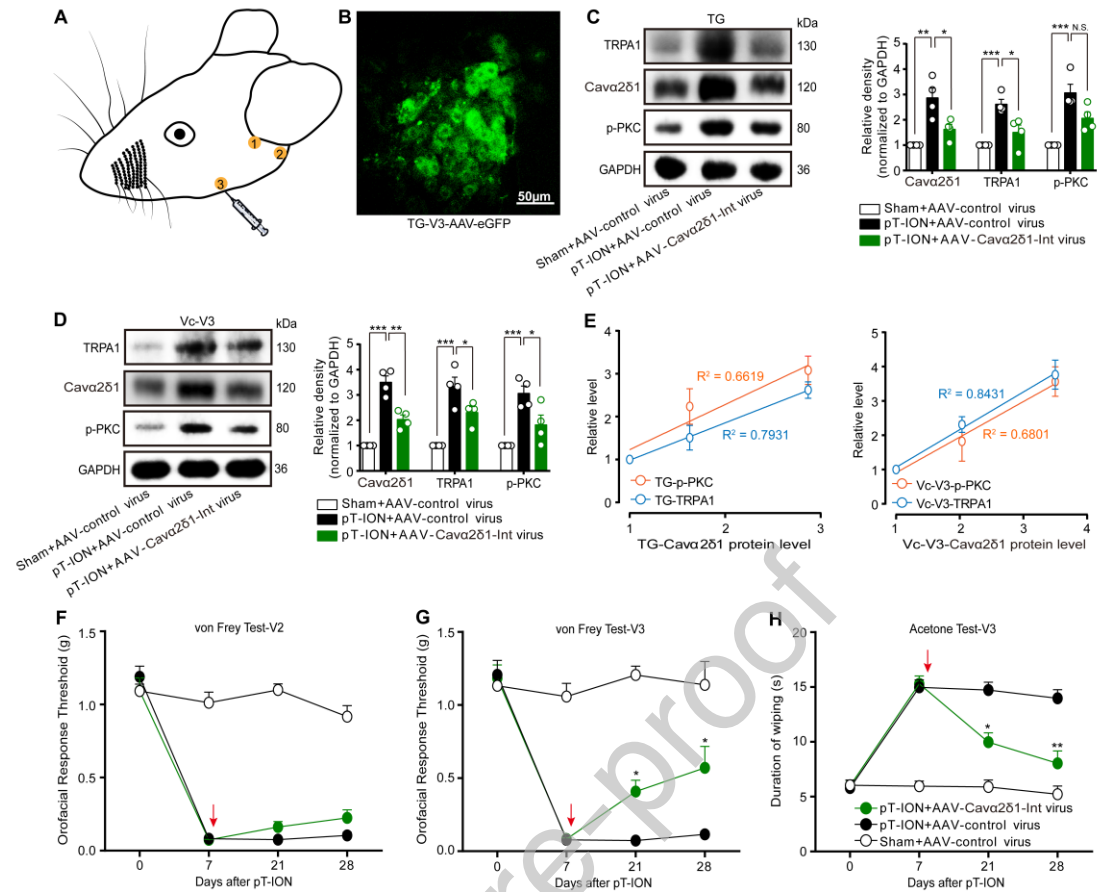


Figure 4. Genetically interfering with the expression of Cavα2δ1 in TG-V3 neurons reversed the upregulation of PKC-TRPA1 and secondary hyperalgesia induced by pT-ION. Mice with established secondary hyperalgesia at 7 days after pT-ION were given a single subcutaneous injection of interfering (Int) (AAV- Cavα2δ1-Int) or control (AAV-control) virus at three sites within the whisker pad V3 area. The injection sites in the TG-V3 area are shown (A). eGFP expression in the TG-V3 neurons following subcutaneous injection of AAV2/6 (B). Scale bar: 50 μm. Knock-down of Cavα2δ1 reversed the increased expression of PKC-TRPA1 induced by pT-ION (C and D). Data are expressed as means ± SEM, n = 4 mice for each group. * $p < 0.05$; ** $p < 0.01$; *** $p < 0.001$ vs. the control group according to one-way ANOVA followed by Tukey's test. The expression of PKC-TRPA1 in the TG and

Vc-V3 was positively correlated with the expression of Cav α 2 δ 1 (**E**, TG-p-PKC: $R^2 = 0.6619$, $p = 0.0013$; TG-TRPA1: $R^2 = 0.7931$, $p = 0.0001$; Vc-V3-p-PKC: $R^2 = 0.6801$, $p = 0.001$; Vc-V3-TRPA1: $R^2 = 0.8431$, $p < 0.0001$). Behavioral tests were performed at the designated time points on the injury side. Knock-down of Cav α 2 δ 1 in TG-V3 neurons attenuated the secondary hyperalgesia but not the primary hyperalgesia (**F-H**). Data presented are the means \pm SEM, $n = 9$ mice for each group. $*p < 0.05$; $**p < 0.01$, compared with the pT-ION+AAV-control virus group according to two-way ANOVA with Sidak's test.

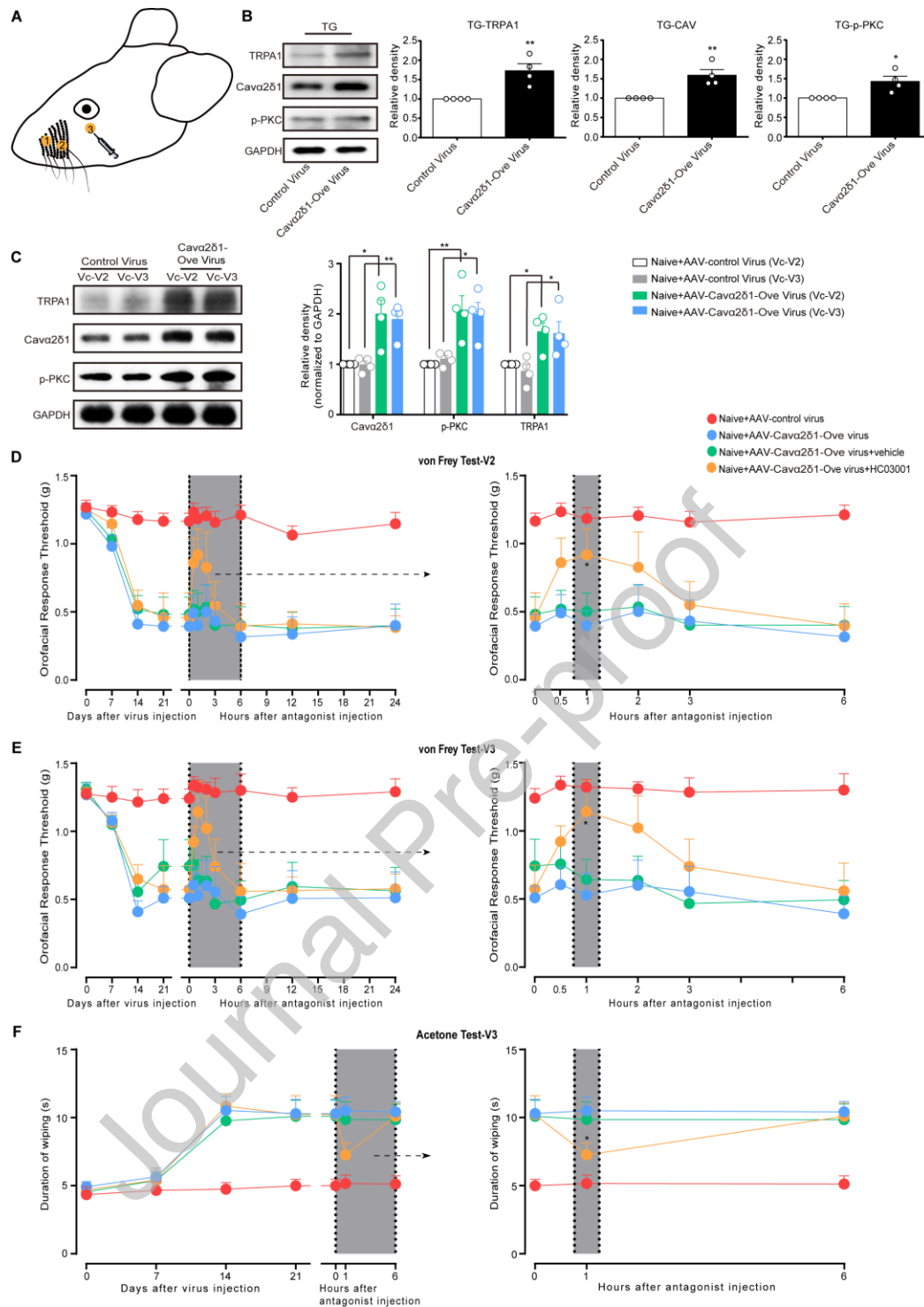


Figure 5. Cava2 δ 1 overexpression in TG-V2 neurons caused PKC-TRPA1-mediated pain hypersensitivity in the whisker pad V2 and V3 areas. The injection sites are shown (A). Cava2 δ 1 overexpression in TG-V2 neurons significantly increased the expression of PKC-TRPA1 in the TG, Vc-V2, and Vc-V3 (B and C). Data are

expressed as means \pm SEM. $*p < 0.05$; $**p < 0.01$ vs. the control group according to Student's t-test (**B**) and one-way ANOVA followed by Tukey's test (**C**), $n = 4$ mice for each group. The time course of changes in mechanical and cold hyperalgesia after a single subcutaneous injection of the Cav α 2 δ 1 overexpression (AAV- Cav α 2 δ 1-Ove) or control (AAV-control) virus into the whisker pad V2 area ($n = 8$ mice in each group) (**D–F, left**). At 21 days after surgery, the systemic administration of the selective TRPA1 receptor antagonist HC-030031 transiently reversed mechanical and cold hypersensitivity induced by Cav α 2 δ 1 overexpression at 1 h after injection. The figures **D–F right** are the expanded views of the grey areas in D–F left. Data are expressed as means \pm SEM. $*p < 0.05$ vs. the respective baselines according to two-way repeated ANOVA analysis.

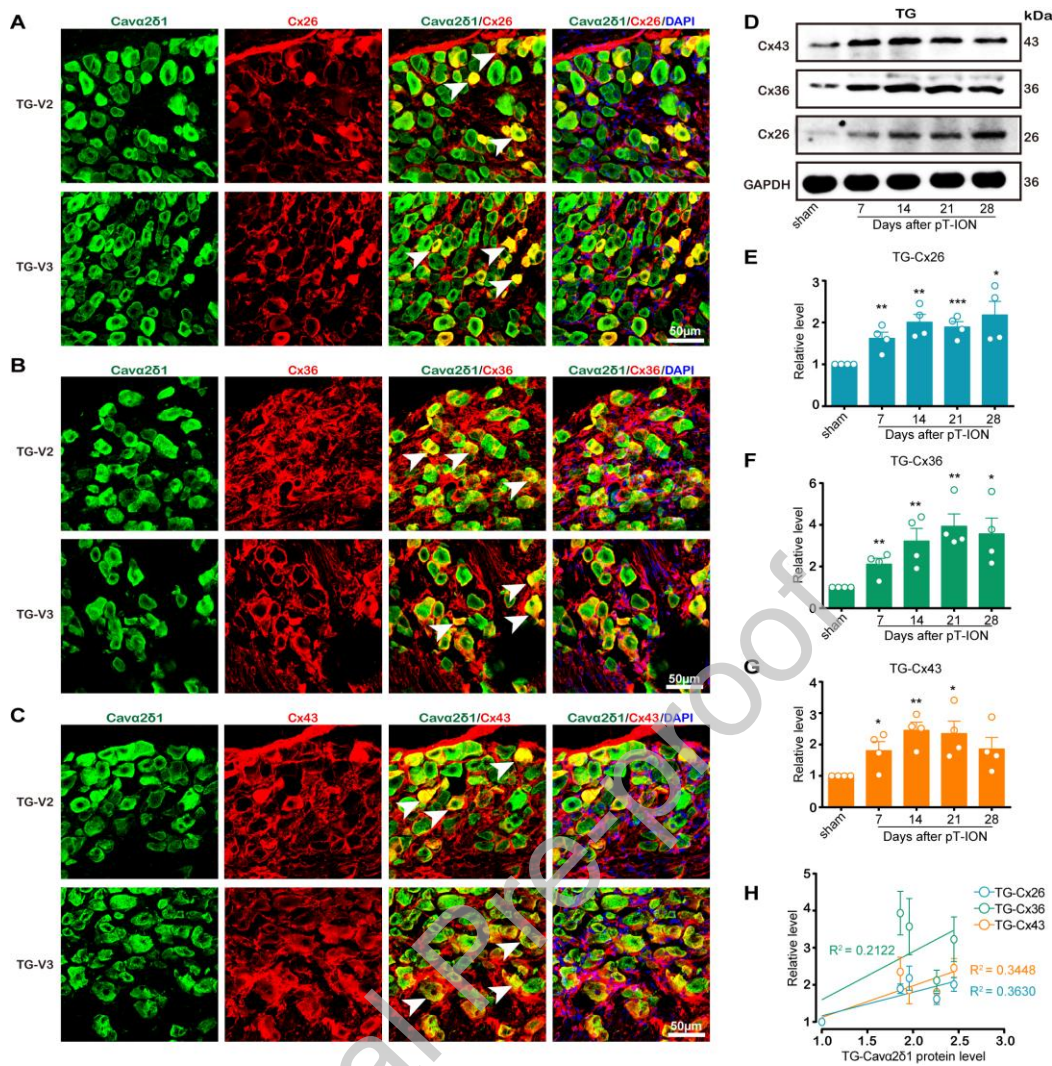


Figure 6. The levels of Cx26, Cx36, and Cx43 protein were significantly increased in the TG after nerve injury. Representative confocal images of colocalization of Cx26, Cx36, and Cx43 with Cava2 δ 1 from the TG-V2 and TG-V3 of pT-ION mice (A–C). Scale bar: 50 μ m. The time course of Cx26, Cx36, and Cx43 protein expression in the TG from sham and pT-ION mice (D–G). The linear correlation between the expression of Cxs and the expression of Cava2 δ 1 in the TG (H, TG-Cx26: $R^2 = 0.3630$, $p = 0.0049$; TG-Cx36: $R^2 = 0.2122$, $p = 0.0409$; TG-Cx43: $R^2 = 0.3448$, $p = 0.0065$). Data presented are the means \pm SEM, $n = 4$ mice for each group. * $p < 0.05$; ** $p < 0.01$; *** $p < 0.001$ vs. the sham group according to one-way ANOVA analysis.

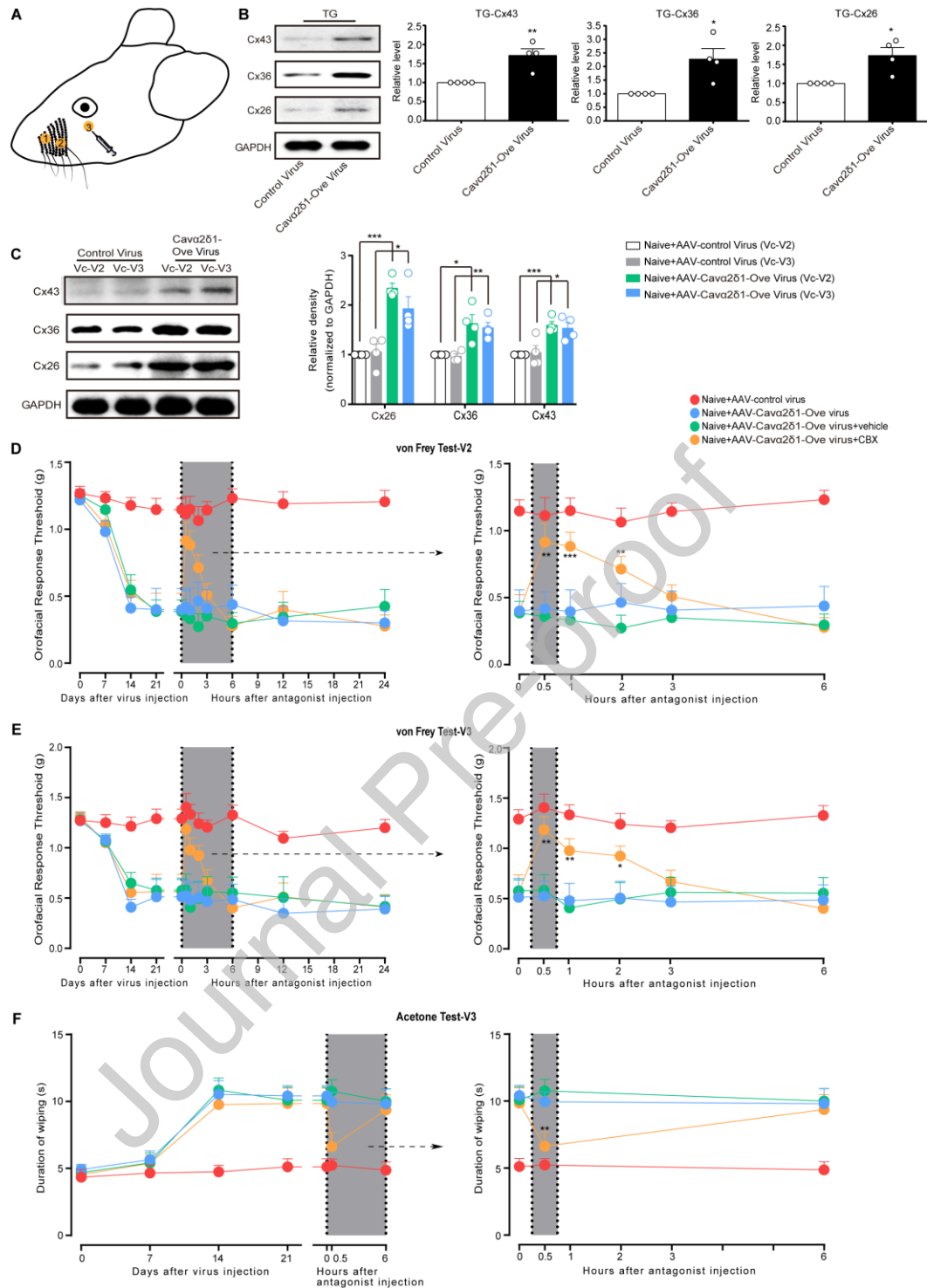


Figure 7. Cava2 δ 1 overexpression in TG-V2 neurons caused GJ-mediated pain hypersensitivity in the whisker pad V2 and V3 areas. The injection sites are shown (A). Cava2 δ 1 overexpression in TG-V2 neurons by AAV-Cava2 δ 1-Ove virus

significantly increased the expression of Cx26, Cx36, and Cx43 in the TG, Vc-V2, and Vc-V3 (**B and C**). Data are expressed as means \pm SEM, $n = 4$ mice for each group. $*p < 0.05$; $**p < 0.01$; $***p < 0.001$ vs. the control group (administered with AAV-control virus) according to Student's *t*-test (**B**) and one-way ANOVA followed by Tukey's test (**C**). Time course of changes in mechanical and cold hyperalgesia after a single subcutaneous injection of the AAV-Cav α 2 δ 1-Ove or AAV-control virus into the whisker pad V2 area (**D–F, left**). At day 21 after surgery, the systemic administration of the GJ blocker CBX (100 mg/kg) transiently reversed mechanical hyperalgesia (starting from 0.5 h lasting to 2 h after drug injection) and cold hyperalgesia (at 0.5 h, the only testing point) induced by Cav α 2 δ 1 overexpression in TG-V2 neurons (**D–F, left**). The Figs **D–F** right are the expanded views of the grey areas in **D–F** left. Data are expressed as means \pm SEM, $n = 8$ mice in each group. $*p < 0.05$; $**p < 0.01$; $***p < 0.001$ vs. the respective baselines according to two-way repeated ANOVA analysis. GJ, gap junction.

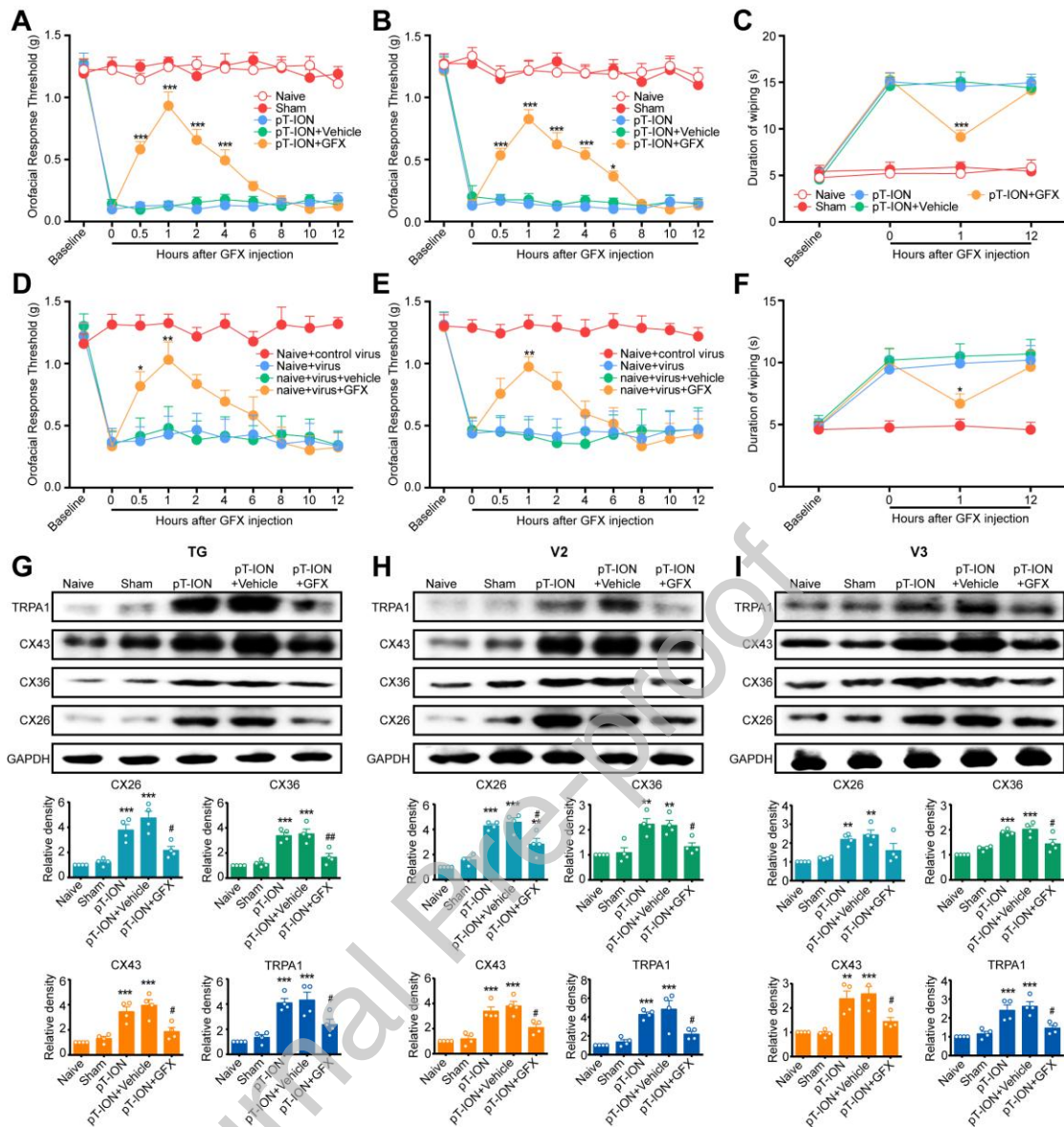


Figure 8. The pain hypersensitivity in the whisker pad V2 and V3 areas and the expression of TRPA1 and GJs induced by nerve injury or Cav α 2 δ 1 overexpression were blocked by PKC blockade. The time course of changes in mechanical and cold hyperalgesia after nerve injury (A–C) and a single subcutaneous injection of the Cav α 2 δ 1 overexpression (Ove) (AAV- Cav α 2 δ 1-Ove) or control (AAV-control) virus into the whisker pad V2 area (D–F). At Day 14 after pT-ION, the systemic administration of the PKC inhibitor GFX significantly reversed mechanical and cold hypersensitivity induced by nerve injury starting from 0.5 h after injection and lasting

for a few hours in both V2 and V3 areas (**A-C**). At Day 21 after surgery, the systemic administration of the PKC inhibitor GFX transiently reversed mechanical and cold hypersensitivity induced by Cav α 2 δ 1 overexpression at 0.5 h and 1 h (V2 and V3) after injection (**D-F**). Data are expressed as means \pm SEM, n = 8 or 9 mice in each group. * p < 0.05; ** p < 0.01; *** p < 0.001 vs. the respective baselines according to two-way repeated ANOVA analysis. The increase in the expression of TRPA1, Cx26, Cx36 and Cx43 in TG (**G**), Vc-V2 (**H**) and Vc-V3 (**I**) was significantly reversed by the PKC inhibitor GFX. Data are expressed as means \pm SEM, n = 4 mice in each group. ** p < 0.01; *** p < 0.001 vs. sham group; # p < 0.05; ## p < 0.01 vs. pT-ION+Vehicle group according to one-way ANOVA analysis.

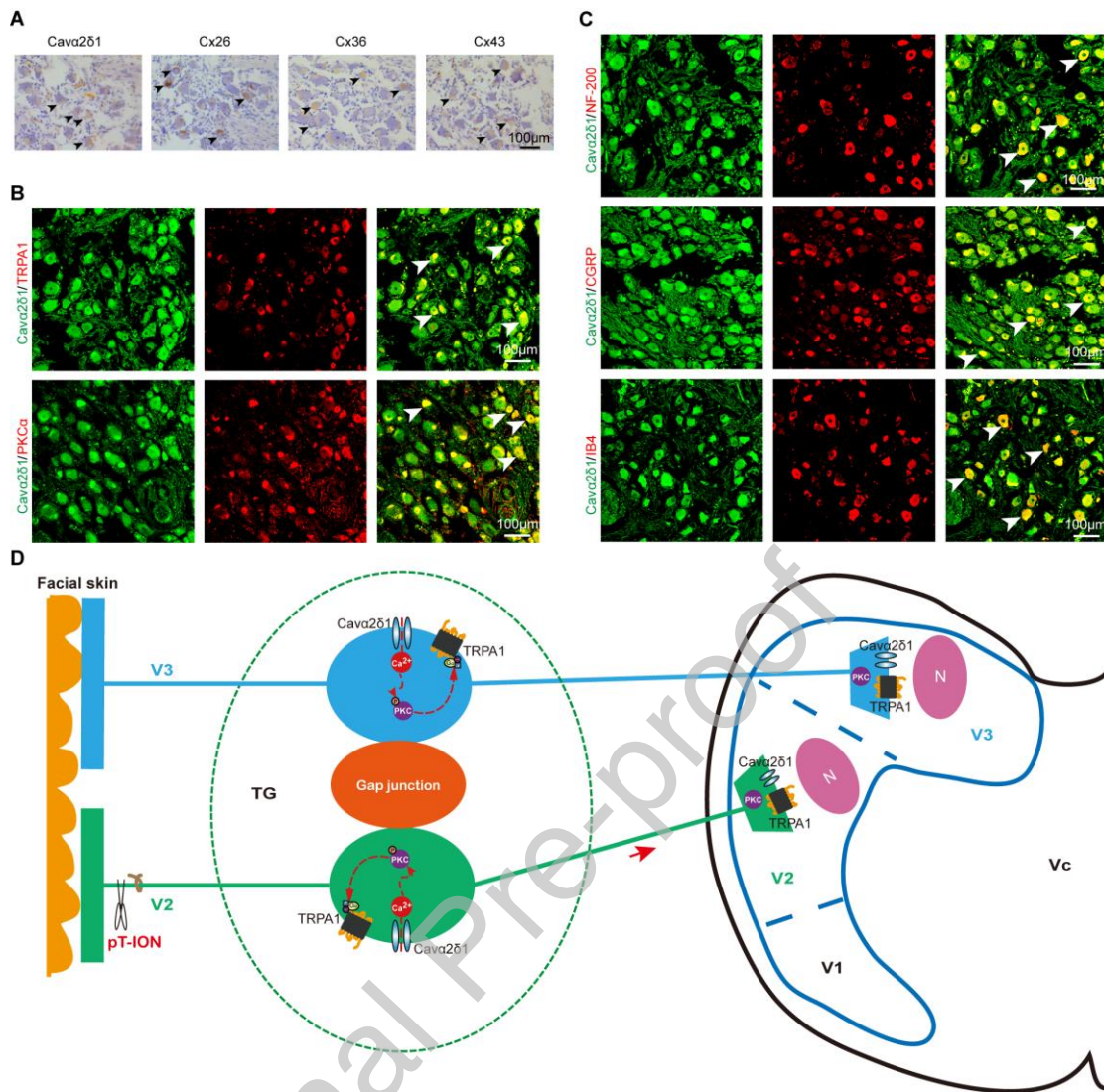
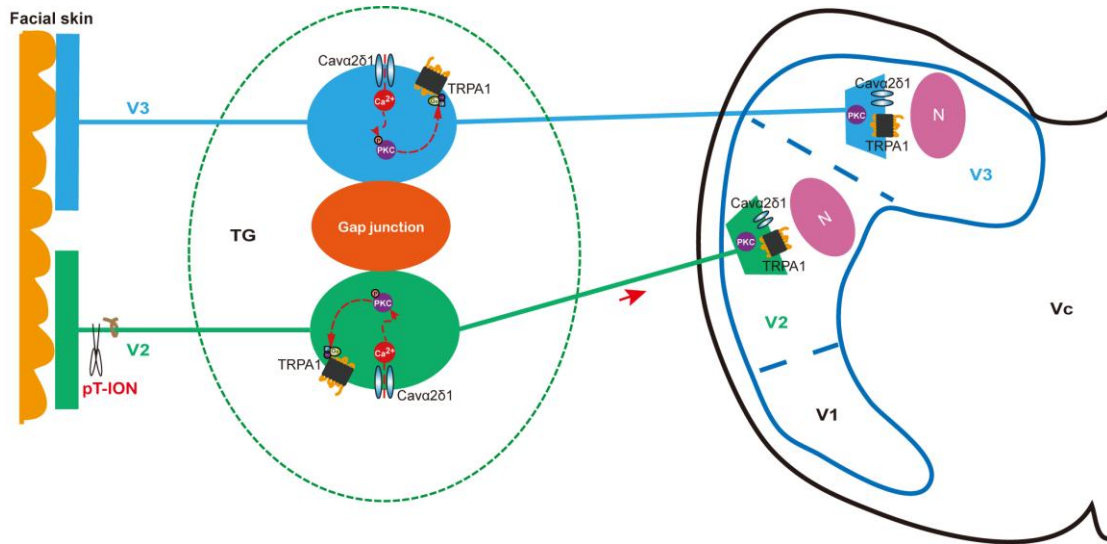


Figure 9. Cavα2δ1, PKC-TRPA1, Cx26, Cx36, and Cx43 were expressed in the human TG. The immunohistochemistry results demonstrated that Cavα2δ1, Cx26, Cx36, Cx43 were expressed in the human TG (A). PKCα and TRPA1 were co-expressed with Cavα2δ1, respectively (B). Cavα2δ1 showed colocalization with the markers (NF200, CGRP, and IB4) of all three types of neurons in the TG (C). Scale bars: 100 μm. Schematic illustration of the proposed mechanism (D). pT-ION induces the upregulation of Cavα2δ1 and the downstream activation of PKC-TRPA1, which leads to hyperactivity of primary TG-V2 subdivision neurons. The nociceptive signal input leads to dorsal horn V2 neuron activation in the Vc, and neuronal

activation then ascends to the thalamus and the cerebral cortex. Meanwhile, the sensitization of TG-V2 neurons subsequently activates the TG-V3 neurons through gap junctions (Cx26, Cx36, and Cx43). Cav α 2 δ 1 and downstream PKC-TRPA1 are activated in both the bodies and central terminals of TG-V3 neurons, resulting in central terminal sensitization of injury nerve fibers and a spread of behavioral hypersensitivity to nearby uninjured facial skin. pT-ION, spared nerve injury of the infraorbital nerve; TG, trigeminal ganglion; Cx, connexin; Vc, trigeminal subnucleus caudalis; N, neuron.



Graphical Abstract